

CHARACTERIZATION OF SORTING NEXIN 3 (SNX3) FUNCTION

A THESIS SUBMITTED TO
THE GRADUATE SCHOOL OF NATURAL AND APPLIED SCIENCES
OF
MIDDLE EAST TECHNICAL UNIVERSITY

BY
MERVE ÖYKEN

IN PARTIAL FULFILLMENT OF THE REQUIREMENTS
FOR
THE DEGREE OF DOCTOR OF PHILOSOPHY
IN
BIOLOGY

JANUARY 2020

Approval of the thesis:

CHARACTERIZATION OF SORTING NEXIN 3 (SNX3) FUNCTION

submitted by **MERVE ÖYKEN** in partial fulfillment of the requirements for the degree of **Doctor of Philosophy in Biology, Middle East Technical University** by,

Prof. Dr. Halil Kalıpçılar
Dean, Graduate School of **Natural and Applied Sciences**

Prof. Dr. Ayşe Gül Gözen
Head of the Department, **Biological Sciences**

Prof. Dr. A. Elif Erson Bensan
Supervisor, **Biology, METU**

Examining Committee Members:

Prof. Dr. Sreeparna Banerjee
Biology, METU

Prof. Dr. A. Elif Erson Bensan
Biology, METU

Prof. Dr. Mesut Muyan
Biology, METU

Assoc. Prof. Dr. Özlen Konu Karakayalı
Molecular Biology and Genetics, Bilkent University

Assist. Prof. Dr. Bahar Değirmenci Uzun
Molecular Biology and Genetics, Bilkent University

Date: 27.01.2020

I hereby declare that all information in this document has been obtained and presented in accordance with academic rules and ethical conduct. I also declare that, as required by these rules and conduct, I have fully cited and referenced all material and results that are not original to this work.

Name, Last name: Merve Öyken

Signature:

ABSTRACT

CHARACTERIZATION OF SORTING NEXIN 3 (SNX3) FUNCTION

Öyken, Merve
Doctor of Philosophy, Biology
Supervisor: Prof. Dr. A. Elif Erson Bensen

January 2020, 90 pages

Sorting nexin 3 (SNX3) belongs to the sorting nexins family involved in endocytic trafficking network. SNX3 only has a PX domain, which facilitates binding to the phosphatidyl inositol-3-phosphate on endosomes and has a role in formation of the retromer complex on early endosomes. Endocytosed receptors go through internalization and recycle back to plasma membrane, Trans-Golgi Network or alternatively are degraded in the lysosomes. Earlier, we found that SNX3 messenger RNA (mRNA) is upregulated via alternative polyadenylation in breast cancers. Therefore, we hypothesized that deregulated expression of SNX3 may change the dynamics of endocytic trafficking of membrane receptors in cancer cells. In order to test our hypothesis, we developed different RNA interference (RNAi) models of SNX3 in cancer cell lines and observed that WLS (Wntless, one of the known cargos of SNX3) and EGFR (Epidermal Growth Factor Receptor, possible cargo of SNX3) levels were altered in SNX3 silenced cells compared with the controls. We used proximity-based ligation approach to demonstrate possible interaction between SNX3 and EGFR, used immunostaining to determine subcellular localization of SNX3 and several mutants we generated that showed deregulated ubiquitylation and abnormal subcellular localization. Overall, we showed that SNX3 modulates EGFR protein levels and that ubiquitylation may be important for SNX3 function.

Understanding the role of SNX3 and the endocytic trafficking may have future implications for targeted therapies against EGFR.

Keywords: Sorting Nexin 3, Epidermal Growth Factor Receptor, Wntless, Cancer, Ubiquitination

ÖZ

SORTING NEXIN 3 (SNX3)'ÜN GÖREVİNİN KARAKTERİZASYONU

Öyken, Merve
Doktora, Biyoloji
Tez Yöneticisi: Prof. Dr. A. Elif Erson Bensan

Ocak 2020, 90 sayfa

Sorting Nexin 3 (SNX3) sorting nexin familyasına ait olan, endositik trafik ağında yer alan bir proteindir. SNX3 sadece PX domainine sahiptir ve bu domain sayesinde endozomlardaki fosfatidil inositol-3-fosfata bağlanır ve retromer kompleksinin erken endozomlarda oluşumunu sağlar. Endositozla hücre içine alınan reseptörler, hücre zarına geri dönebilirler; Trans-Golgi Ağı'na yönlendirilebilirler veya lizozomlarda yıkıma uğrayabilirler. Daha önceki çalışmalarımızda, SNX3'ün mesajcı RNA (mRNA)'sının meme kanserlerinde alternatif poliadenilasyona uğrayarak arttığını göstermiştik. Bu sebeple, düzensiz SNX3 ifadesinin, kanser hücrelerinde hücre zarı reseptörlerinin endositik trafiğinin dinamiklerini değiştirebileceğini hipotez ettik. Hipotezimizi test etmek için, kanser hücre hatlarında SNX3'ün farklı RNA interferaz (RNAi) modelleri geliştirdik. Bu modellerde, WLS (Wntless, SNX3'ün bilinen kargolarından biri) ve EGFR (Epidermal Büyüme Hormonu, SNX3'ün muhtemel kargosu) seviyeleri SNX3'ü baskılanmış hücrelerde, kontrole kıyasla, değişmiştir. Proksimiti ligasyon tekniği kullanılarak, SNX3 ve EGFR arasındaki olası etkileşimi gösterdik. Immunoboyama ile SNX3'ün ve düzensiz ubikutinlenen ve anormal hücre içi lokalizasyon gösteren mutant formlarının hücre içi lokalizasyonlarını belirledik. Özetle, SNX3'ün EGFR

protein seviyesini modüle ettiğini ve ubiquitinlenmenin SNX3'ün fonksiyonunda önemli olabileceğini gösterdik. SNX3'ün görevinin ve endositik trafiğin anlaşılması, EGFR'ye karşı geliştirilecek olan hedefli terapilerde etkili olabilir.

Anahtar Kelimeler: Sorting Nexin 3, Epidermal Büyüme Faktörü Reseptörü, Wntless, Kanser, Ubikutinlenme

To my family,

ACKNOWLEDGMENTS

First and foremost, I would like to express my deepest appreciation to my supervisor Prof. Dr. A. Elif Erson-Bensan for her endless support, motivation, and immense knowledge. Without her inspiring guidance and encouragement, I could not have accomplished this thesis successfully.

I would like to thank all my thesis committee members; Prof. Dr. Sreeparna Banerjee, Prof. Dr. Mesut Muyan, Assoc. Prof. Dr. Özlen Konu Karakayalılar and Assist. Prof. Dr. Bahar Değirmenci Uzun.

I would like to thank to Muyan Lab, Banerjee Lab, Terzi Lab and Gürsel Lab for sharing their resources.

I am extremely grateful to CanSyL (Cancer Systems Biology Laboratory), Prof. Dr. Rengül Çetin Atalay and Dr. Sezen Güntekin for the Nanostring Analysis.

I would like to thank Prof. Dr. Huib Ovaa for allowing me to conduct a part of this study in his laboratory. I specifically appreciate to Dr. Ayşegül Sapmaz for her support and advices.

Many thanks go to all previous and current members of Erson Lab; for providing a fun-filled environment, their precious friendship, and their advices.

I am deeply thankful to my friends for their encouragement, moral support, and suggestions.

Many thanks go to Harun Cingöz for his sincere friendship, support and fun both inside and outside of the lab.

A very special thank is for Ayça Çırçır Hatıl for stimulating discussions, sleepless nights in the lab and all the fun we had during my last five years. Without her help and accompany, I could not have survived.

I would like to thank my cousin Senem Ayşe Haser and my cats Nazlı and Rıfkı for providing me a warm home to accomplish this thesis.

Last but not least, I would like to express my endless gratitude to my family; my mother İncilay Öyken, my father Ethem Öyken, and my brother Uğur Öyken, who are always by my side throughout my life.

I would like to thank TUBITAK for financial support to this study.

TABLE OF CONTENTS

ABSTRACT	v
ÖZ	vii
ACKNOWLEDGMENTS	x
TABLE OF CONTENTS	xii
LIST OF TABLES	xv
LIST OF FIGURES	xvi
LIST OF ABBREVIATIONS	xix
CHAPTERS	
1 INTRODUCTION	1
1.1 Sorting Nexins and Retromer Complex	1
1.1.1 Sorting Nexins	1
1.1.2 Retromer Complex	4
1.2 Sorting Nexin 3 (SNX3)	4
1.2.1 Cargo recognition	6
1.2.2 Post-translational modifications of SNX3	7
1.3 Epidermal Growth Factor Receptor	11
1.4 EGFR and SNXs	14
1.5 Aim of the study	16
2 MATERIALS AND METHODS	17
2.1 Cell lines	17

2.2	Plasmids and siRNAs.....	17
2.3	Site-directed mutagenesis	18
2.4	Transfections.....	19
2.5	EGF treatment.....	19
2.6	Expression analyses	20
2.6.1	RNA isolation	20
2.6.2	DNase I treatment	20
2.6.3	cDNA synthesis	21
2.6.4	TetR expression analysis.....	21
2.6.5	RT-qPCR.....	21
2.7	Western blotting.....	23
2.7.1	Protein isolation	23
2.7.2	Western blotting and antibodies.....	23
2.8	Proximity-based labelling	25
2.9	Flow cytometry	25
2.10	Ubiquitination assay.....	26
2.11	Confocal microscopy	27
2.12	TCF/LEF reporter assay.....	28
3	RESULTS AND DISCUSSION	29
3.1	Silencing of SNX3	29
3.2	The effect of SNX3 silencing on WLS and the Wnt pathway	32
3.3	The effect of SNX3 silencing on the EGFR pathway	37
3.4	The interaction of SNX3 and EGFR	43
3.5	Ubiquitination of SNX3	47

4	CONCLUSION	57
	REFERENCES	61
	APPENDICES	
A.	Buffers and Solutions	73
B.	Vector Maps	77
C.	Markers	81
D.	Sequence results of SNX3 mutants	83
E.	Flow cytometry.....	87
	CURRICULUM VITAE	89

LIST OF TABLES

TABLES

Table 2.1 Primers used for site-directed mutagenesis.....	18
Table 2.2 Primary antibodies used in Western blotting.....	24
Table 2.3 Secondary antibodies used in Western blotting.....	24
Table 2.4 Primary antibodies used in confocal microscopy.....	27

LIST OF FIGURES

FIGURES

Figure 1. 1 Mammalian sorting nexins with their domains.....	2
Figure 1. 2 The retrograde transport of WLS.	5
Figure 1. 3 The consensus VPS26-SNX3 cargo binding motif and the alignment of retromer-binding motifs.....	7
Figure 1. 4 Regulation of recruitment of SNX3 to early endosome.....	9
Figure 1. 5 Schematic view of a ubiquitinated protein.....	10
Figure 1. 6 Schematic view of EGFR signaling pathway.	12
Figure 1. 7 Routes of EGFR.	13
Figure 3. 1 SNX3 levels in stably transfected MDA-MB-231 cells.....	30
Figure 3. 2 The expression of TetR in pcDNA6/TR transfected MDA-MB-231 cells.....	31
Figure 3. 3 SNX3 levels in shRNA transfected MDA-MB-231 cells.	31
Figure 3. 4 Western blot analysis of SNX3 expression in non-target siRNA and SNX3 siRNA transfected MDA-MB-231 cells.....	32
Figure 3. 5 The effect of SNX3 silencing on WLS in MDA-MB-231 cells using a tetracycline-induced system.	33
Figure 3. 6 Western blot analysis of SNX3 and WLS expressions in non-target siRNA and SNX3 siRNA transfected-cells.....	34
Figure 3. 7 TCF/LEF reporter assay in SNX3-silenced MDA-MB-231 cells.....	35
Figure 3. 8 Heatmaps showing the expression of Wnt target genes in MCF10A and MDA-MB-231 cells.....	36
Figure 3. 9 Western blot analysis of SNX3 and CTNNB1 expressions in non-target siRNA and SNX3 siRNA transfected-cells.....	37
Figure 3. 10 Western blot analysis of SNX3 and EGFR expressions in non-target siRNA and SNX3 siRNA transfection different cells.	38
Figure 3. 11 Protein levels of EGFR signaling pathway components in MCF10A and MDA-MB-231 cells.....	39

Figure 3. 12 Relative quantification of EGFR in NT and SNX3 siRNA transfected cells.	40
Figure 3. 13 The effect of SNX3 silencing on EGFR in MDA-MB-231 cells using a tetracycline-induced system.	41
Figure 3. 14 Western blot analysis of SNX3 and EGFR expressions of stably NT and SNX3 shRNA transfected MDA-MB-231 and HeLa cells.	42
Figure 3. 15 Biotinylation of SNX3 and its interactants.	44
Figure 3. 16 Biotinylation of SNX3 and its interactions with EGFR after EGF treatment.	45
Figure 3. 17 Cell surface EGFR levels determined by flow cytometry on EGF-treated HeLa cells.	46
Figure 3. 18 Ubiquitination status of SNX3 and its mutated versions.	48
Figure 3. 19 Ubiquitination status of SNX3 with EGF treatment.	49
Figure 3. 20 Ubiquitination status of SNX3 and its mutated versions with EGF treatment.	50
Figure 3. 21 Confocal microscopy images of SNX3-GFP WT and its mutant forms.	51
Figure 3. 22 Confocal microscopy images of SNX3-GFP WT and SNX3-GFP K95R mutant.	54
Figure 3. 23 Confocal microscopy images of EGF-treated SNX3-GFP WT and SNX3-GFP K95R mutant.	55
Figure B. 1 Vector map of pSUPER.retro.neo+GFP.	77
Figure B. 2 Vector map of pSUPERIOR.retro.neo+GFP.	78
Figure B. 3 Vector map of pcDNA6/TR.	78
Figure B. 4 Vector map of pcDNA 3.1 (-).	79
Figure B. 5 Vector map of pEGFP-N1.	80
Figure C. 1 Protein ladder (Thermo PageRuler Plus Prestained, Cat #: 26619).	81
Figure C. 2 DNA Ladder (Thermo GeneRuler 100 bp Plus, Cat #: SM0321).	82

Figure D. 1 Sequence result of SNX3-GFP K61-63R mutant.....	83
Figure D. 2 Sequence result of SNX3-GFP K95R mutant.....	84
Figure D. 3 Sequence result of SNX3-GFP K119R mutant.....	85
Figure D. 4 Sequence result of SNX3-GFP K128R mutant.....	86
Figure E. 1 Gating strategy of the flow cytometry analysis.	87

LIST OF ABBREVIATIONS

ABBREVIATIONS

AKT	AKT serine/threonine kinase
AMPA	α -amino-3-hydroxy-5-methyl-4-isoxazolepropionic acid
AP2	adaptor protein-2
APP	Amyloid precursor protein
AREG	Amphiregulin
ARP2/3	actin-related protein-2/3
β 2AP	Beta-2-adrenergic receptor
BAR	Bin, amphiphysin, Rvs
BTC	Betacellulin
CI-MPR	cation-independent mannose 6-phosphate receptor
CME	Clathrin-mediated endocytosis
DAPI	Diamidino-2-phenylindole
DUB	Deubiquitinating enzyme
Dvl	Dishevelled
EEA1	Early endosome antigen 1
EGF	Epidermal growth factor
EGFR	Epidermal growth factor receptor
EMT	Epithelial-to-mesenchymal transition
EPG	Epigen
ER	Endoplasmic Reticulum
EREG	Epiregulin
ERK	Extracellular signal-regulated kinase
F	Phenylalanine
FEEL-1	fasciclin/epidermal growth factor (EGF)-like/laminin-type EGF-like/link domain-containing scavenger receptor-1
Fz	Frizzled

GAP	GTPase activating protein
GAPDH	Glyceraldehyde 3-phosphate dehydrogenase
GFP	Green fluorescent protein
GIT1	GPCR kinase-2 interacting protein 1
GM130	Golgin A1
GPCR	G-protein coupled receptor
HBEGF	Heparin-binding EGF-like
IP	Immunoprecipitation
K	Lysine
L	Leucine
LAMP1	Lysosomal Associated Membrane Protein 1
LDLR	Low-density lipoprotein receptor
LRP1	LDRL-related protein 1
M	Methionine
NCE	Non-clathrin endocytosis
NT	Non-targeting
PBS	Phosphate buffered saline
PCR	polymerase chain reaction
PLC γ 1	Phospholipase C gamma 1
PM	Plasma membrane
PtdIns(3)P or PI3P	Phosphatidyl-inositol-3-phosphate
PTM	Post-translational modification
PX	Phox-homolgy
R	Arginine
RAB5	Ras-Related Protein Rab-5A
RPLP0	Ribosomal protein lateral stalk subunit P0
shRNA	Short-hairpin RNA
siRNA	Small-interfering RNA
SNX	Sorting nexin
TBC1D5	Tre-2/Bub2/Cdc16 [TBC]1 domain-containing 5

TetR	Tetracycline repressor
TfR	Transferrin receptor
TGF α	Transforming growth factor-alpha
TGN	Trans-Golgi Network
TNBC	Triple negative breast cancer
Ub	Ubiquitination/Ubiquitin
VAPA	VAMP Associated Protein A
VPS	Vacuolar protein sorting
W	Tryptophan
WCL	Whole-cell lysate
WLS	Wntless
WT	Wild-type
Y	Tyrosine
ZO2	Zonula occludens 2

CHAPTER 1

INTRODUCTION

1.1 Sorting Nexins and Retromer Complex

1.1.1 Sorting Nexins

Sorting nexins (SNXs) are a group of proteins containing Phox-homology (PX) domain.¹ All SNX proteins have PX domain, but some of them have additional domains and are classified accordingly. For example, SNX-BAR group members have a C-terminal BAR (Bin, amphiphysin, Rvs) domain. Other SNX proteins contain only the PX domain. The last group has other recognized domains in addition to the SNX-PX domain, many of which are involved in cell signaling (Figure 1.1).²

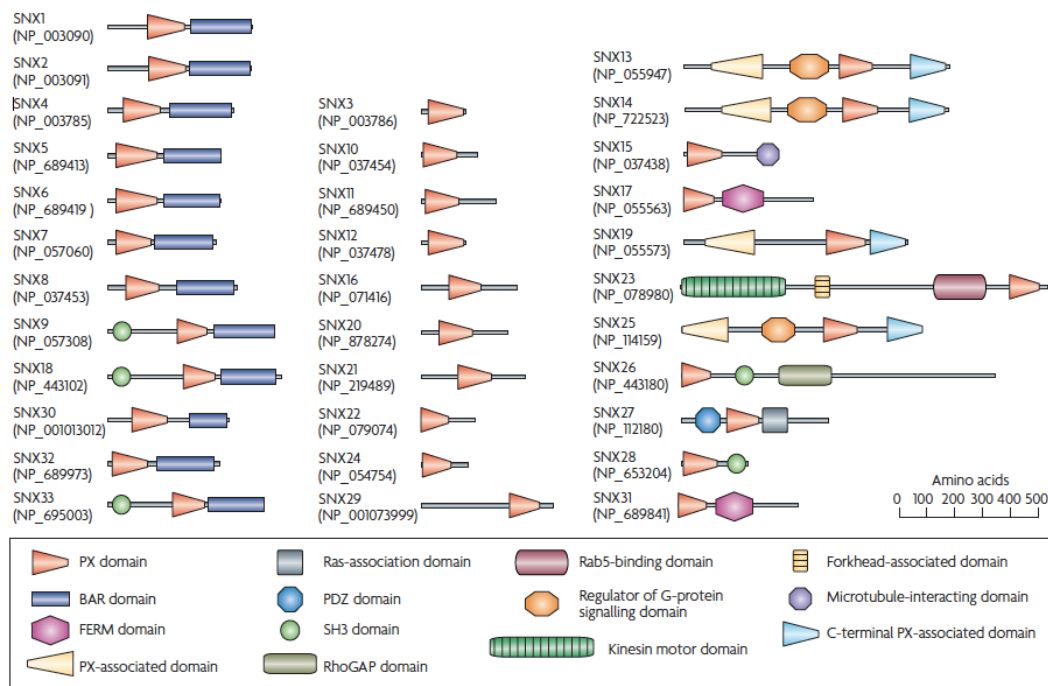


Figure 1. 1 Mammalian sorting nexins with their domains. FERM, protein 4.1, ezrin, radixin, moesin; PDZ, postsynaptic density protein-95, Discs-large, Zona-occludens-1; RhoGAP, Rho GTPase-activating protein; SH3, Src-homology-3.²

All of the SNX-PX domains have >50% sequence homology with the PX domain of SNX1, except the PX domain from SNX26.³ PX domain is required to bind the SNX proteins to early endosomal membranes containing phosphatidylinositol-3-monophosphate (PtdIns3P). Through their interaction with endosomes, SNXs have diverse functions in endocytosis, endosomal sorting, and endosomal signaling.⁴

SNX-BAR subfamily members can form specific homo- and heterodimers due to their BAR domains.⁵ Due to their structure and arrangement, BAR domains can bind to curved membranes.⁶ The members of this group are well characterized and involved in various cellular processes. SNX9, SNX18, and SNX33 have roles in endocytosis.⁷ SNX4 is needed for transport from early to recycling endosomes.⁸ SNX8 is required in traffic of the endosome-to-Trans Golgi network (TGN).⁹ SNX5-SNX6 heterodimer has roles in the transport of cargo proteins with carriers along microtubules.¹⁰

SNXs containing the FERM-like domain are SNX17 and SNX31. The role of FERM domains is mediating interactions of cytoskeletal elements or membranes with cytosolic proteins.¹¹ This domain interacts with other proteins containing the "NPXY" motif.¹² With this sorting signal in their cytoplasmic tails of cargo proteins, SNX17 functions in endosome-to-plasma membrane recycling of some of the transmembrane proteins. These proteins that need SNX17 for their recycling are the low-density lipoprotein receptor (LDLR)^{13,14} and LDLR-related protein 1 (LRP1)¹⁵, the endothelial cell adhesion molecule P-selectin¹⁶, fasciclin/epidermal growth factor (EGF)-like/laminin-type EGF-like/link domain-containing scavenger receptor-1 (FEEL-1)¹⁷, amyloid precursor protein (APP)¹⁸ and β -integrins.^{19,20} Unlike traditional retromer-mediated sorting, SNX17 works with different proteins called "Retriever complex and Commander assembly" to sort its cargo.²¹ One of the least characterized SNX proteins is SNX31. It binds to integrins and modulates their expressions on cell surface.²²

SNX27 is the only protein containing a PDZ domain. It can interact with other proteins through a PDZ-binding motif at the C-terminus of cargo proteins. Beta-2-adrenergic receptor (β 2AR) was the first cargo protein that was found to interact with SNX27 and retromer for endosome-to-plasma membrane recycling.²³ Other cargo proteins of SNX27 are the α -amino-3-hydroxy-5-methyl-4-isoxazolepropionic acid (AMPA) receptor²⁴, a potassium channel Kir3.3²⁵ and the epithelial tight junction component zonula occludens 2 (ZO2).²⁶

SH3-domain-containing SNX9 has a very distinct role when compared to other SNX proteins. It binds to clathrin, cargo adaptor protein-2 (AP2), dynamin and the actin-related protein-2/3 (ARP2/3)-complex activator N-WASP, and mediates plasma-membrane remodeling events.²⁷ It is attracted to PtdIns(4,5)P2-enriched plasma membrane and regulates the dynamin-mediated membrane fission step of endocytosis.²⁸

In summary, different domains of SNX family members provide distinct functions within the endomembrane trafficking.

1.1.2 Retromer Complex

The retromer complex is a protein complex localized to endosomes and conserved in eukaryotes.²⁹ Earlier, the function of mammalian retromer was stated as a regulator of endosome-to-TGN transport of the lysosomal hydrolase receptor cation-independent mannose 6-phosphate receptor (CI-MPR).^{30,31} Later, it was shown that retromer also functions in the transport of other receptors. In addition to the plasma membrane (PM)-TGN path, retromer complex has roles in the recycling of receptors from endosomes to PM.³² Because retromer complex maintains the homeostasis of different receptors in cells, retromer mutations have been linked to diseases including late-onset Parkinson's in some patients^{33,34} and Alzheimer's.³⁵

Biochemical and structural studies revealed the complexity of the retromer. It constitutes three core proteins: Vps35, Vps29, and Vps26 (Vacuolar protein sorting). Vps35 is the largest component of retromer and it creates a scaffold for Vps26 and Vps29 to bind and make a heterotrimer in a 1:1:1 ratio.³⁶ Vps29 is the smallest component of the complex. With the help of conserved residues on Vps29, it interacts with the C-terminus of Vps35.^{37,38} Mammalian Vps26 has two paralogues (Vps26A and Vps26B) and they bind to Vps35 at its N-terminus.³⁹ Retromer itself cannot bind to the endosome. Therefore, retromer interacts with many proteins during membrane recruitment and cargo recognition. Small GTPase Rab7 is required for the association of retromer to endosomes.⁴⁰ The interaction of retromer with Rab7 is transient because GTPase activating protein (GAP) TBC1D5 (Tre-2/Bub2/Cdc16 [TBC]1 domain-containing 5) switch Rab7 from GTP-bound to GDP-bound state.⁴¹ Retromer is also associated with SNX proteins for membrane remodeling and cargo selectivity.

1.2 Sorting Nexin 3 (SNX3)

SNX3 is a member of SNX proteins containing only the PX domain. SNX3 is not able to form heteromeric forms with other SNXs since it lacks coiled-coil domains.⁴²

Because of its PX domain, SNX3 is a phosphatidyl-inositol-3-phosphate (PtdIns(3)P)-binding protein.⁴³ SNX3, with the help of Rab7, is an essential protein for the recruitment of retromer complex to early endosomes.⁴⁴

SNX3 is involved in the retrograde transport of Wntless (WLS) from early endosomes to Golgi.^{45,46} WLS is a transmembrane protein responsible for the carrying of Wnt proteins from Endoplasmic Reticulum (ER) to the plasma membrane. After the release of Wnt ligands outside of the cell, WLS is internalized.⁴⁷ Endocytosed WLS firstly meets with SNX3-containing early endosomes. After the recruitment of retromer, the SNX3-retromer complex sorts its cargo (WLS) to TGN. In the absence of SNX3, WLS is missorted and undergoes lysosomal degradation (Figure 2).⁴⁵ Moreover, silencing of SNX-BAR orthologues (SNX1-SNX2 and SNX5-SNX6) did not affect the sorting of WLS in *C. elegans* and *Drosophila*. Therefore, SNX3 is the only known responsible SNX protein for the trafficking of WLS.⁴⁵

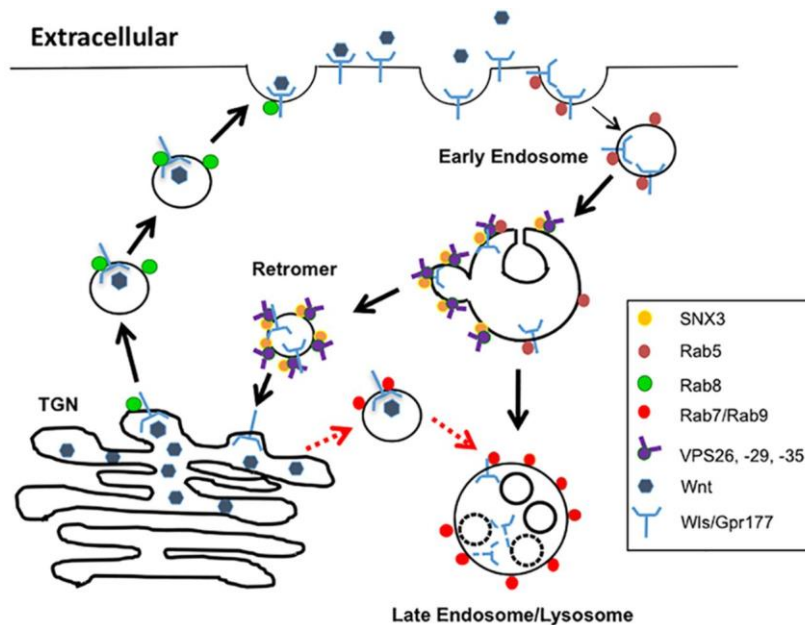


Figure 1. 2 The retrograde transport of WLS. Wnt ligands are attached to WLS and carried to the plasma membrane for secretion. The empty WLS proteins are endocytosed and SNX3-retromer sorts them to Golgi.⁴⁸

When a Wnt ligand binds to the seven-pass transmembrane Frizzled (Fz) receptor and its co-receptor, low-density lipoprotein receptor-related protein 6 (LRP6), or its close relative LRP5, the Wnt pathway is activated. The formation of Wnt-Fz-LRP6 complex recruits the scaffolding protein Dishevelled (Dvl) resulting in LRP6 phosphorylation and activation and the recruitment of the Axin complex to the receptors. These events lead to inhibition of Axin-mediated β -catenin phosphorylation. As a result, β -catenin is stabilized, accumulates and travels to the nucleus to form complexes with TCF/LEF and activates Wnt target gene expression.⁴⁹ Increased activity of β -catenin (*CTNNB1*) is detected in many cancer types.⁵⁰ However, mutations to explain increased β -catenin levels or mutations in other components of the Wnt pathway are not common in breast cancers.

SNX3 also involves in the recycling of the transferrin receptor (TfR). The cycle of TfR in cell begins with the internalization of Tfr into early endosomes with SNX3. SNX3-retromer directs the sorting of Tfr from early endosomes to recycling endosomes. Sec1511 mediates the transport of Tfr from recycling endosomes to the plasma membrane. The silencing of SNX3 causes hemoglobin defects and anemia in vertebrates because of the degulated iron uptake through TfR. Absence of SNX3 also results in accumulation of TfR in early endosomes.⁵¹ Moreover, without SNX3, retromer complex cannot even bind to endosomal membranes.²⁹

1.2.1 Cargo recognition

X-ray crystallographic analyses revealed that SNX3 interacts with N-terminus of VPS35 and C-terminus of VPS26 through its N-terminus. VPS29 only interacts with C-terminus of VPS35.³⁹ When these interactions occur, conformational changes of the SNX3-retromer complex reveals a binding pocket for cargo. Cargo proteins bind this pocket with the help of their recycling signals. It was shown that these cargo proteins share a common motif in its C-terminal tail: $\emptyset X(L/M)$ in which \emptyset stands for bulky amino acids such as Tyrosine (Y), Tryptophan (W), and Phenylalanine (F);

L stands for amino acid Leucine, and M stands for amino acid Methionine. Later, this motif was expanded with recent studies.⁵² Figure 1.3 shows this motif in detail.

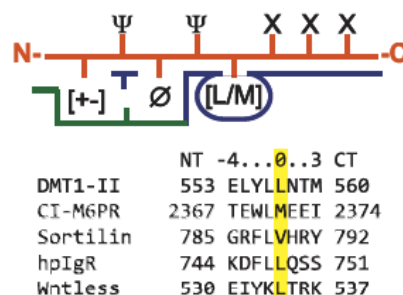


Figure 1. 3 The consensus VPS26-SNX3 cargo binding motif and the alignment of retromer-binding motifs. X stands for any residue, Ø a bulky aromatic residue, Ψ a residue having a hydrophobic or long aliphatic hydrocarbon tail, and [+/-] any charged residue.⁵²

Given its role in cargo recognition, SNX3 may be an important retromer protein that is responsible for the recycling of membrane receptors that carry the ØX(L/M) motif.

1.2.2 Post-translational modifications of SNX3

Post-translational modifications (PTMs) are reversible chemical modifications of proteins modifying the fate of proteins. Modified proteins are altered in terms of degradation, signaling, and interactions with other proteins.⁵³ PTMs can occur at any time in a life-cycle of a protein. Most of the proteins are modified after their translation for their appropriate folding or their cellular localization. Some proteins are modified after their folding and localization. These modifications may affect their activities, making them active or inactive in a cellular event. In addition, proteins can be tagged for degradation.⁵⁴

PTMs occur at specific amino acid residues or peptide linkages and enzymes are involved in most of these processes. These enzymes are ligases, phosphatases,

kinases and transferases making more than 200 different modifications. Most common PTMs are phosphorylation, acetylation, methylation, ubiquitination, SUMOylation, glycosylation and prenylation.⁵⁵

Phosphorylation is one of the most widely studied PTMs. It mediates various cellular processes, such as differentiation, apoptosis and cell growth.⁵⁶ Tyrosine, serine, and threonine are amino acids that are commonly phosphorylated in mammalian cells.⁵⁷ Kinases are responsible for phosphorylation, and phosphatases are the enzymes that dephosphorylate proteins. These enzymes work together in a balanced state to regulate phosphorylation of proteins.⁵⁸ Deregulation in phosphorylation can cause severe diseases like cancers. Mutated kinases and phosphatases can disrupt this balance and can activate or de-activate cancer-related genes.⁵⁹ Phosphorylation contributes to change the affinity of proteins to other proteins by changing the conformation of the phosphorylated protein. Enzymes can be activated or de-activated. It can also tag proteins for degradation.⁶⁰

According to a recent study, SNX3 is a phosphorylated protein.⁶¹ When serine 72 (Ser72) of SNX3 is phosphorylated, SNX3 cannot bind to PI3P on early endosomes (Figure 1.4). The study suggests that the addition of a negatively charged group inhibits the binding. In addition, since Arginine 70 on SNX3 is one of the amino acids responsible for PI3P recognition, phosphorylation of SNX3 on Ser72 may prevent this recognition. They generated constitutively non-phosphorylated (S72A) and phosphorylated (S72E) mutants of SNX3 and observed that S72A mutant localized on endosomes, while S72E mutant retained in the cytosol. This site is conserved among many species including invertebrates, vertebrates, fungi, and plants. Phosphorylation is also observed among other SNX proteins. Ser188 on SNX1⁶² and Ser73 on SNX12⁶³ are the phosphorylation sites and mutations on these sites resulted in the same effect as SNX3. Deregulation of this PTM was also observed in cancer. Hyperphosphorylation of SNX3 was recorded in neuroblastoma⁶⁴, breast cancer⁶⁵, leukemia⁶⁶ and lymphoma.⁶⁷

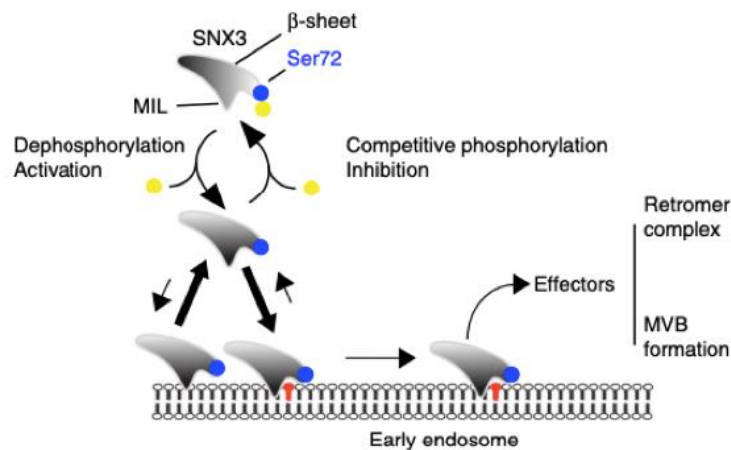


Figure 1. 4 Regulation of recruitment of SNX3 to early endosome. Phosphorylation on Ser72 inhibits and dephosphorylation activates the binding of SNX3 on PI3P. MIL: membrane insertion loop, MVB: Multi-vesicular bodies.⁶¹

Ubiquitination is another PTM that directs proteins for proteasomal or lysosomal degradation, but it has many diverse roles in cellular processes, such as mediating protein-protein interactions, transcriptional regulation, and DNA repair.⁶⁸ This modification is an ATP-dependent reaction and carried out with 3 classes of enzymes (Figure 1.5). Ubiquitin-activating enzyme E1 binds ubiquitin to ubiquitin-conjugating enzyme E2. Ubiquitin ligase enzyme E3 binds this ubiquitin to a lysine residue of the substrate protein. Multiple additions of ubiquitin results in targeting protein for degradation.⁵⁴

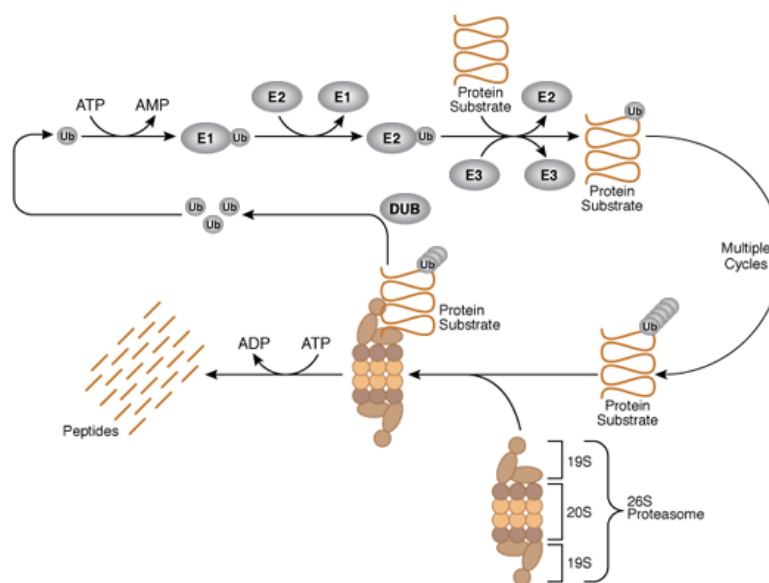


Figure 1. 5 Schematic view of a ubiquitinated protein. E1, E2, and E3 enzymes work together to add ubiquitin to substrate protein.⁶⁹

There are two types of protein ubiquitination named according to the number of ubiquitin attachment: monoubiquitination and polyubiquitination. Polyubiquitination is made of ubiquitin chains constructed by E1, E2 and E3 enzymes due to the nature of ubiquitin. It contains 7 lysine residues at positions 6, 11, 27, 29, 33, 48, and 63, allowing the addition of ubiquitin to another ubiquitin.⁶⁸ Polyubiquitin chains added through Lysine 48 (Lys48) is for proteasomal degradation.⁷⁰ Lys11-linked chains are also reported for proteasomal degradation.⁷¹ Lys63 chain is responsible for DNA damage repair, kinase activation, endocytosis, and signal transduction.⁷² Monoubiquitination has more diverse roles than polyubiquitination. One of them is affecting membrane protein trafficking. Many cell surface proteins are internalized to the endocytic pathway through monoubiquitination.⁷³ Histone proteins H2A and H2B are monoubiquitinated which is important for gene expression during development and meiosis.⁷⁴ The addition of ubiquitin to proteins can be removed by deubiquitinases (deubiquitinating enzyme, DUBs), making these regulations even more complex.⁵⁴

There is so far only one study that reported SNX3 to be ubiquitinated.⁷⁵ SNX3 was shown to interact with USP10 (a deubiquitinating enzyme) that SNX3 degradation is decreased when USP10 is expressed in HEK293 cells. Therefore, USP10 may be the DUB that removes ubiquitin from SNX3, leading to inhibition of degradation. However, ubiquitination sites of SNX3 and consequences of ubiquitination are not fully understood yet.

1.3 Epidermal Growth Factor Receptor

Epidermal growth factor receptor (EGFR, HER1, ErbB1) is a member of the ErbB receptor tyrosine kinase family. This family has 3 more members: ErbB2 (HER2), ErbB3 (HER3) and ErbB4 (HER4).⁷⁶ EGFR signaling has crucial roles, such as adult tissue regeneration and developmental processes at the systematic level; and proliferation, migration, and survival at the cellular level.⁷⁷ Deregulation of EGFR signaling and genetically changed *EGFR* gene results in several cancers: lung, colon, breast, glioblastoma, etc. Therefore, EGFR is an important target in cancer therapies.⁷⁸

EGFR signaling is a very complicated pathway due to the different ligands and their different outcomes. Seven known EGFR ligands are present: epidermal growth factor (EGF), transforming growth factor- α (TGF α), amphiregulin (AREG), epiregulin (EREG), heparin-binding EGF-like (HBEGF), betacellulin (BTC), and epigen (EPG).⁷⁹ TGF α , AREG, EPG, and EGF (best-characterized EGFR ligand) only bind to EGFR, but the others also bind to ErbB4. These different ligands have different binding kinetics to EGFR, and affect the EGFR trafficking differently.⁸⁰

After ligand binding, EGFR dimerizes and initiates signaling cascades. There are 3 main signaling cascades activated: PI3K/AKT, MAPK/ERK and PLC γ 1 (Figure 1.6).⁸¹

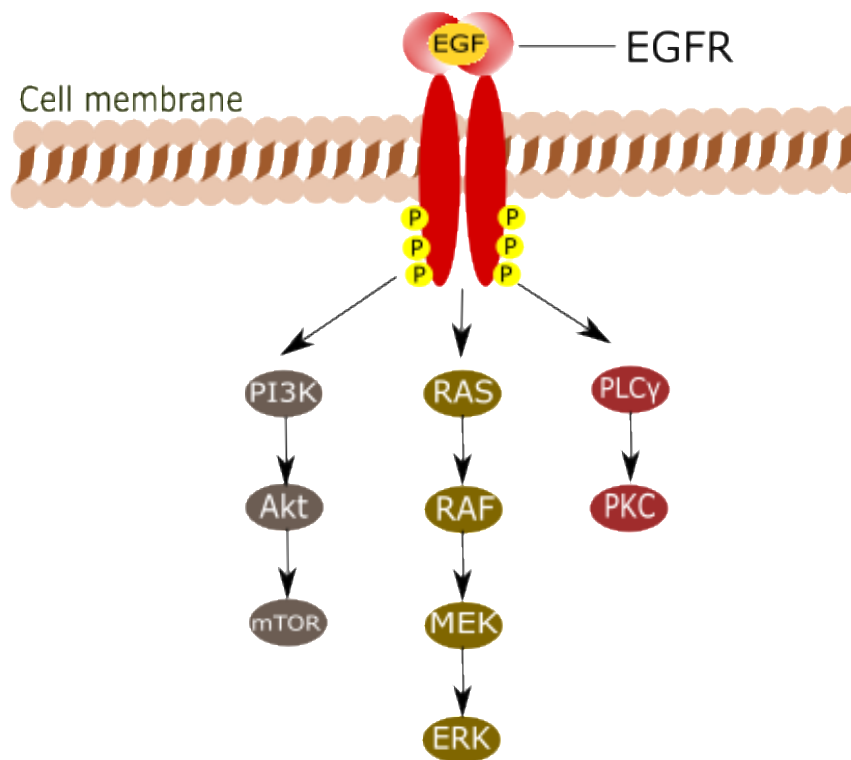


Figure 1. 6 Schematic view of EGFR signaling pathway. Binding of EGF activates EGFR signaling with triggering EGFR phosphorylation. Major signaling cascades are activated, such as PI3K/AKT, MAPK/ERK and PLC γ 1. These cascades resulted in tumor formation, cell proliferation and migration.

EGFR protein can be examined in five parts: an extracellular region for ligand recognition, a transmembrane domain, an intracellular region including the juxtamembrane regulatory region, the kinase domain-containing lysine residues for receptor ubiquitination, and the intracellular C-terminal regulatory tail that contains the tyrosine residues phosphorylated upon ligand binding.^{82,83}

Structural studies revealed the activation of EGFR at the plasma membrane. In the absence of ligand, EGFR rests in an inactive state. In this state, receptor dimerization and kinase activity are not observed.⁸⁴ However, some spontaneous dimerization can occur without ligand binding, but receptor activation does not happen.⁸⁵ Upon ligand binding, EGFR changes its conformation due to the dimerization of the receptor. This structural change is transmitted to the cytoplasmic tail. Each monomer trans-autophosphorylates the specific tyrosine residues on the other monomer's

cytoplasmic tail and eventually signaling cascade initiates.⁷⁶ Following phosphorylation, EGFR endocytosis is triggered. Endocytosis can occur in two different ways: clathrin-mediated endocytosis (CME) and non-clathrin endocytosis (NCE) (Figure 1.6). The selection of the endocytic route depends on the cellular context, ligand type and concentration, and homo- or hetero-dimerization.

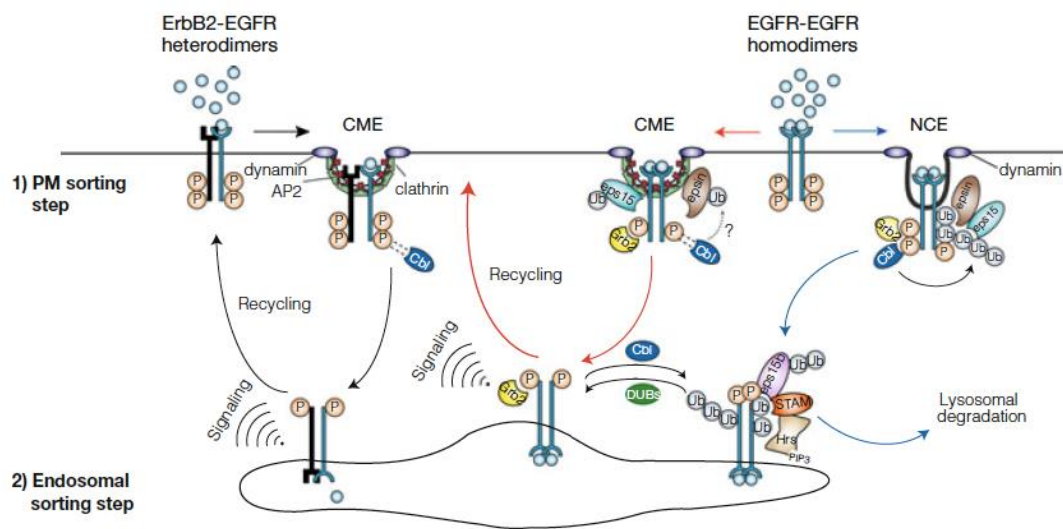


Figure 1. 7 Routes of EGFR. ErbB2-EGFR heterodimers internalize through CME and recycle back to the plasma membrane. EGFR homodimers can internalize through both CME and NCE. It can be degraded in lysosome or recycle back under different conditions.⁸⁶

ErbB2-EGFR heterodimers are auto-phosphorylated upon ligand binding. They are endocytosed through CME with the help of clathrin, AP2, and other adaptor proteins. The ubiquitination of this type of dimer is poor due to the inefficient recruitment of Cbl (an E3 ligase that ubiquitinates lysine residues in the kinase domain of EGFR).⁸⁷ In the endosomal sorting step, ligand dissociates from the dimer due to the acidic environment in endosomes. ErbB2-EGFR heterodimers are recycled back to plasma membrane.⁸⁸

EGFR-EGFR homodimers can internalize through CME and NCE. Ligand concentration affects this choice. High, saturating concentrations of EGF (>10 ng/ml) leads to clathrin-independent endocytosis, increased ubiquitination and eventually leads to lysosomal degradation of most of the EGFR (>90%).⁸⁹ Clathrin-dependent endocytosis occurs in all ligand concentrations, but the recycling of EGFR occurs at a higher rate (70%) and degradation of EGFR takes place at a lower rate (30%). CME affects EGFR signaling in many ways. In limited ligand concentrations, CME protects EGFR from degradation and sustains EGFR signaling. It also recycles EGFR back to the plasma membrane where EGFR is needed.⁹⁰ In contrast, NCE favors receptor degradation in high ligand concentration. This route may protect the cell from over-stimulated EGFR signaling. Deregulation of NCE results in tumorigenesis, resulting in uncontrolled EGFR signaling without EGFR degradation.⁹¹

1.4 EGFR and SNXs

As part of the retromer complex, numerous SNX proteins have been implicated in EGFR endocytic processes, specifically for lysosomal sorting. For example, SNX1 binds to a specific site on EGFR to target it for lysosomal degradation. Consequently, Overexpression of SNX1 leads to a decrease of EGFR on the cell surface of HEK293 cells and increased degradation in lysosomes. The localization of SNX1 and EGFR is not known.⁹²

SNX2 is also involved in lysosomal degradation of EGFR. It is co-localized with EGFR in HeLa and LNCaP cells. PX-domain mutated SNX2 failed to localize with EGFR and inhibited the EGFR degradation. Although SNX2 localizes in early endosomes, the localization of SNX1 and EGFR has not been clear yet.⁹³

SNX6 interacts with G-protein coupled receptor (GPCR) kinase-2 interacting protein 1 (GIT1) to sort EGFR from endosomes to the lysosome. GIT1 and SNX6 localize together in early endosomes. The knockdown of GIT1 decreased EGF-induced

EGFR degradation. As expected, overexpression of both GIT1 and SNX6 enhanced EGF-induced EGFR degradation in pulmonary artery smooth muscle cells.⁹⁴

EGF-induced EGFR degradation was also increased with SNX16 overexpression, suggesting the role of SNX16 in lysosomal degradation.⁹⁵ SNX16 was shown in early and transferrin receptor-positive recycling endosomes. It also immunoprecipitated with EGFR after EGF induction in COS7 cells.

SNX10 also co-localizes with EGFR in early endosome upon EGF treatment in HeLa cells, but the effect of this interaction is unknown.⁹⁶

Overexpression of SNX5 inhibits degradation of EGFR in NR6 cells through an unknown mechanism.⁹⁷ In addition, SNX5 inhibits endocytosis and degradation of EGFR in hepatocellular carcinoma cells.⁹⁸

The role of cargo recognition of SNXs proteins has been identified for BAR domain-containing SNX5-SNX6, FERM domain containing SNX17, and PDZ domain-containing SNX27. SNX5/6-SNX1/2 heterodimers recognize the $\Phi x \Omega x \Phi(x)_n \Phi$ motif on the cytosolic tails of their cargo proteins with the PX domain of SNX5. C-terminal FERM domain of SNX17 and retriever complex recognize NPx[FY]/Nxx[FY] motif and [ED][ST]x Φ motif is required for the sorting of receptor proteins with SNX27 and retromer complex.^{99,100} SNX3 has also been shown to be important in cargo recognition. Cargoes containing $\emptyset X[L/M]$ motif on their cytoplasmic tails were found to be sorted by SNX3 and retromer complex.⁵²

Interestingly, same cargo protein can be recognized by different SNX proteins to carry it to same destination in the cell. For example, CI-MPR (mannose 6-phosphate receptor) contains both $\Phi x \Omega x \Phi(x)_n \Phi$ and $\emptyset X[L/M]$ motifs for its recognition by SNXs. SNX1/2-SNX5/6 without retromer complex carries CI-MPR to TGN with Golgin-245 tethering¹⁰¹, while SNX3 with retromer complex does the same function with Golgin GCC88 tethering.¹⁰² These findings reveal the complexity of receptor trafficking in the cells.

Given the information of cargo proteins regulated with different SNXs, EGFR may also be a cargo protein of SNX3. We found the SNX3 recognition motifs on EGFR using motif analysis tools, suggesting that SNX3 may involve in EGFR trafficking.

EGFR is an important RTK with paradoxical roles in breast cancers. EGFR-amplified primary breast tumors were shown to be highly proliferative with EGF induction and they were sensitive to EGFR inhibition. Conversely, after these cells became metastatic due to the epithelial-to-mesenchymal transition (EMT), EGF induction led to growth inhibition. In addition, the metastatic form of this tumor was resistant to EGFR inhibitors such as Gefitinib (EGFR-specific kinase inhibitor).¹⁰³ This paradox makes the treatment of patients difficult. Triple negative breast cancer (TNBC) is defined as highly metastatic, poor patient prognosis and difficult to treat due to the absence of estrogen, progesterone and HER2 receptors, which are targeted in other types of BCs.¹⁰⁴ Therefore, EGFR becomes an important target and gains importance for TNBCs because of its high expression in this cancer type.

Overexpression of SNX3 delays the degradation of EGFR in A431 cells, leading the accumulation of endocytosed EGFR in early endosomes.⁴³ Consistently, silencing of SNX3 resulted in decreased protein level of EGFR in A431 and HeLa cells.¹⁰⁵ Therefore, considering our initial observation on SNX3 and its cargo recognition potential, we focused on SNX3 in BCs.

1.5 Aim of the study

Earlier, our group reported alternative polyadenylation of SNX3 in TNBC patients.¹⁰⁶ Given its unique role in cargo recognition and retromer recruitment, we were interested whether SNX3 may have a role in breast cancers and hypothesized that deregulated expression of SNX3 may alter recycling dynamics of cancer related PM receptors, specifically EGFR.

CHAPTER 2

MATERIALS AND METHODS

2.1 Cell lines

MCF10A (human non-tumorigenic breast cancer cell line) cells were grown in DMEM/F12 medium with 5% horse serum, 1% Penicillin/Streptomycin (P/S), 100 mg/ml EGF, 1 mg/ml hydrocortisone, 1 mg/ml cholera toxin, and 10 mg/ml insulin. MDA-MB-231 (human triple-negative breast cancer cell line), HeLa (human cervical adenocarcinoma cell line) and HEK293 (human embryonic kidney cell line) cells were grown in DMEM high glucose medium supplemented with 10% Fetal Bovine Serum (FBS) and 1% P/S. MDA-MB-468 (human triple-negative breast cancer cell line) cells were grown in DMEM high glucose medium supplemented with 10% FBS, 1% non-essential amino acids and 1% P/S. All cell lines were grown as monolayers and incubated at 37°C with 95% humidified air and 5% CO₂.

2.2 Plasmids and siRNAs

Coding sequence of SNX3 was cloned into pEGFP-N1 (a kind gift from Dr. Volkan Seyrantepe, İzmir Institute of Technology-Turkey). EGFR-GFP vector (cat# #32751) were purchased from Addgene. pcDNA3.1-TurboID-HA vector was a kind gift from Dr. Mesut Muyan (Middle East Technical University, Turkey). Coding sequence of SNX3 was cloned into pcDNA3.1-TurboID-HA vector and pcDNA3.1-SNX3-TurboID-HA vector was created. SNX3 short-hairpin RNA (shRNA) (5'-AAGGGCTGGAGCAGTTTATAA-3') and non-targeting (NT) shRNA (5'-CGTACGCGGAATACTTCGATT-3') were cloned into pSUPER retro.neo-GFP (a kind gift from Dr. Uygur Tazebay, Gebze Technical University-Turkey). For

inducible silencing, same shRNAs were cloned into pSUPERIOR retro.neo-GFP (a kind gift from Dr. Yasemin Eraç, Ege University-Turkey). pcDNA 6/TR (a kind gift from Dr. Uygur Tazebay, Gebze Technical University-Turkey) were used for the expression of tetracycline repressor.

SNX3 small-interfering RNA (siRNA) (SMARTpool: siGENOME M-011521-01, Dharmacon) and NT siRNA (Qiagen, cat# 1027310) were used in transient silencing of SNX3. DharmaFect (Dharmacon, cat# T-2004) was used to transfect siRNAs.

2.3 Site-directed mutagenesis

pEGFP-SNX3 construct was used to generate SNX3 mutants. Specific primers were designed to change the Lysine of interest into Arginine (Table 2.1). pEGFP-SNX3 construct was used as template in the polymerase chain reaction (PCR). DpnI enzyme (Thermo Scientific, Cat #: ER1701) was used to digest the methylated constructs in PCR product. The remaining unmethylated constructs were transformed into TOP10 *E. Coli* competent cells and amplified. Thermo GeneJET Plasmid Mini Prep Kit was used to isolate vectors according to manufacturer's instructions. Mutants were verified by sequencing (Appendix D).

Table 2.1 Primers used for site-directed mutagenesis.

Primer name	Sequence (5'-3')
K61-63R_F	AGGGTCAAGACAAATCTTCCTATTTTCAGGCTGAGAGAATCTACTGTTAG
K61-63R_R	CTAACAGTAGATTCTCTCAGCCTGAAAATAGGAAGATTTGTCTTGACCCCT
K95R_F	TTCCCCCGCTCCCTGGGAGAGCGTTTTTG
K95R_R	CAAAAACGCTCTCCCAGGGAGCGGGGAA
K119R_F	GACAATTTTATTGAGGAAAGAAGACAAGGGCTGGAGCAGTT
K119R_R	AACTGCTCCAGCCCTTGTCTTCTTTCCTCAATAAAATTGTC
K128R_F	GGCTGGAGCAGTTTATAAACAGGGTCGCTGGTC
K128R_R	GACCAGCGACCCTGTTTATAAACTGCTCCAGCC

2.4 Transfections

Vectors were amplified in TOP10 *E. coli* bacteria. Thermo GeneJET Plasmid Mini Prep Kit was used to isolate vectors according to manufacturer's instructions. Vectors were quantified in Maestrogen Nano. For stable transfections, cells were seeded to 6-well plates. Next day, 2 µg of vectors was transfected using 4 µl of Turbofect transfection reagent. After 24 hours of transfection, antibiotic was given to eliminate the untransfected cells. pcDNA6/TR transfected MDA-MB-231 cells were selected using 5.5 µg/ml of blasticidine S hydrochloride (Sigma, Cat #: 15205). MDA-MB-231 and HeLa cells transfected with pSUPER and pSUPERIOR constructs were selected using 1000 µg/ml and 800 µg/ml G418 (Merck, Cat #: 04727878001), respectively. Antibiotic concentrations were reduced by half after all untransfected cells were died. Monoclonal and polyclonal cells were selected and transfection efficiency was controlled. Transient transfections were performed using indicated vectors and Turbofect transfection reagent for indicated times.

SNX3 siRNA (SMARTpool: siGENOME M-011521-01, Dharmacon) and NT siRNA (Qiagen, Cat #: 1027310) were used in transient silencing of SNX3. DharmaFect (Dharmacon, Cat #: T-2004) was used to transfect siRNAs. Transfection success was controlled with Western blotting.

2.5 EGF treatment

For EGF treatments, EGF (Gibco, Cat #: PHG0313) was used as indicated concentrations. Prior to treatment, HeLa cells were serum-starved in DMEM containing no serum for 3 hours. Then, EGF was given to cells in this serum-free DMEM in indicated times. For confocal microscopy, Alexa-Fluor 647 labelled EGF (Invitrogen, cat#: E35351) was given as described above.

2.6 Expression analyses

2.6.1 RNA isolation

Total RNA was isolated using High Pure RNA Isolation Kit (Roche, Cat #: 11828665001) according to manufacturer's instructions.

2.6.2 DNase I treatment

DNase treatment was performed to eliminate genomic DNA in isolated RNAs. 10 µg of RNA was incubated with 5 µl of DNase I (Merck, Cat #: 047167280-01), 10 µl of 10X DNase incubation buffer and RNase-DNase-free ultra-pure water (Biological Industries, Cat #: BI01-866-1A) up to 100 µl for 1 hour at 37°C. 100 µl of phenol-chloroform-isoamylalcohol was added to stop the reaction. Samples were vortexed for 30 seconds and incubated on ice for 10 minutes. They were centrifuged in cold, 14000 rpm centrifuge to separate RNAs. Upper phases were collected, and 240 µl of cold 100% EtOH and 8 µl of 3 M sodium acetate were added to precipitate RNA. Samples were incubated at -20°C overnight. Next day, RNAs were collected using 14000 rpm-cold centrifuge for 30 minutes. RNA pellets were washed with cold 70% EtOH and centrifuged again for 15 minutes. RNA pellets were air-dried and suspended with ultra-pure water. The quality and quantity of RNAs were determined using Maestrogen Nano.

To check the efficiency of DNase treatment, RNAs were used as template in the PCR using GAPDH (Glyceraldehyde 3-phosphate dehydrogenase) specific primers. GAPDH_F: 5'-GGGAGCCAAAAGGGTCATCA-3' and GAPDH_R: 5'-TTTCTAGACGGCAGGTCAGGT-3' (product size: 409 bp). Following conditions were used for the PCR reactions: incubation at 94°C for 10 minutes, 35 cycles of 94°C for 30 seconds, 56°C for 30 seconds, and 72°C for 30 seconds, and final extension at 72°C for 10 minutes. Genomic DNA was used as a positive control.

2.6.3 cDNA synthesis

RevertAid First Strand cDNA Synthesis Kit (Thermo Fisher Scientific, Cat #: LSG-K1622) were used. 1 µg of RNA was incubated with 1 µl of oligo dT and ultra-pure water up to 12 µl at 65°C for 5 minutes. 4 µl of reaction buffer, 2 µl of 10 mM dNTPs, 1 µl of Ribolock (RNase inhibitor) and 1 µl of reverse transcriptase were added to samples. They were incubated at 42°C for 1 hours and then at 70°C for 5 minutes. cDNAs were stored in -20°C.

2.6.4 TetR expression analysis

TetR (tetracycline repressor) expression is required for some of the inducible shRNA systems. TetR expression was determined by RT-PCR using the genomic DNAs of stably pcDNA6/TR transfected MDA-MB-231 cells. Following primers were used; TetR_F: 5'-AACAACCCGTAAACTCGCCC-3' and TetR_R: 5'-TCTCAATGGCTAAGGCGTCG-3' (product size: 120 bp). Incubation at 94°C for 10 minutes, 30 cycles of 94°C for 30 seconds, 56°C for 30 seconds, and 72°C for 30 seconds, and final extension at 72°C for 5 minutes.

2.6.5 RT-qPCR

For RT-qPCR, SYBR® Green Mastermix (Bio-Rad, Cat #: 1725121) was used using the CFX Connect (Bio-Rad) cycler. 10 µL reactions were performed with 300 nM of specific primer pairs. *EGFR* was amplified using the following primer pair: EGFR_F: 5'-GCGTCCGCAAGTGTAAGAAG-3', EGFR_R: 5'-CCACTGATGGAGGTGCAGTT-3' (product size: 136 bp). The fold change was normalized against reference gene Ribosomal Protein Lateral Stalk Subunit P0 (*RPLP0*)¹⁰⁷, amplified with the following primer pair: RPLP0_F: 5'-GGAGAAACTGCTGCCTCATA-3', RPLP0_R: 5'-GGAAAAAGGAGGTCTTCTCG-3' (product size: 191 bp). For all reactions,

following conditions were used: incubation at 94°C for 10 minutes, 40 cycles of 94°C for 15 seconds, 60°C for 30 seconds, and 72°C for 30 seconds. For the relative quantification, the reaction efficiency incorporated $\Delta\Delta C_q$ formula was used.¹⁰⁸ Student t-test was performed using GraphPad Prism (California, USA).

2.6.6 NanoString Analysis

Complementary DNA synthetic oligos were used in NanoString Technology in order to bind, capture and tag mRNA molecules for counting. It does not require DNase treatment, reverse transcription or amplification of RNAs. RNAs were isolated as mentioned above. Three independent siRNA transfections were performed and RNAs were pooled and loaded in three replicates. 100 ng of total RNA was loaded for each sample into the cartridge nCounter® Vantage 3D™ Wnt Pathways Panel. nSolver software of NanoString Technologies were used to assess the quality of the run and process data. Microsoft Excel was used to analyze data and GraphPad Prism 8 was used to draw graphs and further statistical analysis. Two normalization analyses were done as recommended by manufacturer to generate normalized counts. First normalization includes six internal positive controls that are run in each cartridge. Their geometric means were calculated and a normalization factor was obtained to equilibrate each count of each gene to this normalization factor. In the second normalization, the same process was applied to each gene, but using the geometric mean of housekeeping genes (CC2D1B, COG7, EDC3, GPATCH3, HDAC3, MTMR14, NUBP1, PRPF38A, SAP130, SF3A3, TLK2, ZC3H14). Advanced Analysis Module was used to analyze the data in terms of specific biological processes.

2.7 Western blotting

2.7.1 Protein isolation

Total protein was isolated using M-PER Mammalian Protein Extraction Reagent (Thermo, Cat#: 78501). Cytoplasmic and nuclear protein isolation was performed using NE-PER Nuclear and Cytoplasmic Extraction Reagents (Thermo, Cat#: 78835). Isolations were done according to manufacturers' protocol. PhosSTOP (Roche, Cat#: 04906837001) and protease inhibitor (Roche, Cat#: 1187350001) were added to M-PER to prevent phosphorylation and degradation of proteins, respectively. Protein concentrations were measured using Pierce BCA Protein Assay Kit (Thermo, Cat#: 23227) according to manufacturer's protocol. Isolated proteins were stored in -80°C.

2.7.2 Western blotting and antibodies

50 µg of protein extracts were boiled with 6X Laemmli Buffer (Appendix A) at 95°C for 10 minutes and loaded to 10% SDS-polyacrylamide gel. After the separation of proteins, they were transferred onto PVDF membrane (Merck, cat# 03010040001). Either skim-milk (BioRad Blotting-Grade Blocker, cat# 170-6404) or bovine serum albumin (BSA; Serva, cat# 11943.01) were used for blocking in TBS-T (Appendix A). Membranes were incubated overnight at 4°C with appropriate primary antibodies and 1 hour at room temperatures with appropriate HRP-conjugated secondary antibodies. For the visualization of proteins, WesternBright ECL (Advansta, cat# K12045-D50), Chemidoc MP Imaging System (BioRad) and Odyssey Classic imager (LI-COR) were used.

Primary antibody information was listed in Table 2.2.

Table 2.2 Primary antibodies used in Western blotting.

Protein name	Source	Catalog number and brand	Blocking buffer	Dilution
SNX3	rabbit	10772-1-AP, ProteinTech	5% BSA in 1%TBS-T	1:500
EGFR	mouse	sc-373746, SCB	5% SM in 1% TBS-T	1:500
EGFR ⁺	rabbit	06-847, Millipore	5% SM in 1% TBS-T	1:1000
WLS	mouse	655902, BioLegend	5% BSA in 1%TBS-T	1:500
pY ⁺	mouse	05-321, Millipore	5% SM in 1% TBS-T	1:1000
p-EGFR	rabbit	2220, CST	5% BSA in 1%TBS-T	1:500
p-PLC γ 1	rabbit	14008, CST	5% SM in 1% TBS-T	1:1000
PLC γ 1	rabbit	5690, CST	5% BSA in 1%TBS-T	1:500
p-AKT	rabbit	4060, CST	5% BSA in 1%TBS-T	1:1000
AKT	rabbit	sc-8312, SCB	5% SM in 1% TBS-T	1:500
p-ERK 1/2	rabbit	sc-16982, SCB	5% SM in 1% TBS-T	1:500
ERK 1/2	mouse	sc-514312	5% BSA in 1%TBS-T	1:200
CTNNB1	mouse	sc-133240	5% SM in 1% TBS-T	1:500
HA ⁺	mouse	MMS-101R, Covance	5% SM in 1% TBS-T	1:1000
GFP ⁺	rabbit	REF ¹⁰⁹	5% SM in 1% TBS-T	1:1000
HDAC1	mouse	sc-81598	5% SM in 1% TBS-T	1:1000
TUBA1B*	mouse	HRP-66031, ProteinTech	5% SM in 1% TBS-T	1:5000
GAPDH*	rabbit	sc-25778, SCB	5% SM in 1% TBS-T	1:2000
ACTB	mouse	sc-47778, SCB	3% BSA in 1%TBS-T	1:4000
ACTB ⁺	mouse	A5441, Sigma Aldrich	5% SM in 1% TBS-T	1:10000

BSA: Bovine serum albumin, SM: Skim milk, SCB: SantaCruz Biotechnology, CST: Cell Signaling Technology. Antibodies with ⁺ and * signs were used in Ovaa Lab and borrowed from Banerjee Lab, respectively.

Secondary antibody information was listed in Table 2.3.

Table 2.3 Secondary antibodies used in Western blotting.

Antibody name	Catalog number and brand	Dilution
Goat-anti-mouse HRP	R-05071, Advansta	1:4000
Goat-anti-rabbit HRP	R-05072, Advansta	1:4000

IRDye 800CW goat anti-rabbit IgG (H + L)*	926-32211, Li-COR	1:5000
IRDye 800CW goat anti-mouse IgG (H + L)*	926-32210, Li-COR	1:5000
IRDye 680LT goat anti-rabbit IgG (H + L)*	926-68021, Li-COR	1:20000
IRDye 680LT goat anti-mouse IgG (H + L)*	926-68020, Li-COR	1:20000

Antibodies with * signs were used in Ovaab Lab.

2.8 Proximity-based labelling

HeLa or HEK293 cells were transfected either with pcDNA3.1-TurboID-HA or pcDNA3.1-SNX3-TurboID-HA vectors. Next day, 50 μ M biotin (Sigma, Cat# B4639) was given to cells for 4 hours. Lysis buffer (Appendix A) was used to lyse cells and samples were incubated at 4°C with rotation for 20 min. Lysates were centrifuged for 20 min at full speed (14000 rpm) and 4°C. 0.5% SDS and High Capacity Neutravidin beads (Thermo Scientific, Cat# 29202) were added to supernatants of samples and incubated by rotating at 4 °C for overnight. Wash buffer (lysis buffer containing 0.5% SDS) was used for washing the beads for 4 times with 300xg centrifugation for 5 min. After removal of all the supernatant, sample loading buffer (Appendix A) containing 10 mM DTT was added to beads and they were boiled at 95°C for 15 min. Whole cell lysates with sample loading buffer (Appendix A) containing 20 mM DTT were boiled at 95°C for 10 min. Then, lysates were loaded to 8% SDS-PAGE and appropriate antibodies were used to detect the proteins.

2.9 Flow cytometry

HeLa cells were seeded to T75 flasks. 5 ng/ml and 12 μ g/ml CHX were given to cells for overnight and 4 hours. During the 4 hours CHX treatment, cells were serum-starved. Then, cells were treated with either 5 ng/ml or 25 ng/ml EGF for indicated times. After washing with PBS, 1X citrate buffer (Appendix A) was used to collect the cells. Cells were centrifuged and counted. For each sample, 2 million cells were added to tubes. Cells were washed with cold cell staining buffer (Appendix A) for 4

times with cold centrifugation. For blocking, cold 5% BSA in PBS were used and cells were incubated on ice for 30 min. After washing with cold cell staining buffer for 4 times, cells were either incubated with allophycocyanin-labeled anti-EGFR (BioLegend, Cat #: 352905) or isotype control (BioLegend, Cat #: 400121) antibodies in blocking buffer for 45 min. at 4°C in the dark. After centrifugation, PBS were added to cells and analyzed using BD Accuri C6 flow cytometer (BD Biosciences).

2.10 Ubiquitination assay

Ubiquitination status of GFP-tagged proteins was assessed by using ubiquitination assay.¹¹⁰ HEK293 cells was seeded to 6 cm-dishes. Next day, they were transfected with HA-ubiquitin, SNX3-GFP wild-type and its mutants as indicated. After 24 hours of transfection, they were lysed in 300 μ L lysis buffer 1 containing 10mM N-methyl maleimide (general DUB inhibitor diluted in DMSO, freshly added) (Appendix XXX) and protease inhibitors (Roche Cat#: 1187350001, freshly added) by scraping. Then, 100 μ L lysis buffer 2 (Appendix A) were added to the crude lysates; samples were sonicated (Fisher Scientific FB120 Sonic Dismembrator, 3 pulses, amplitude 40%) and SDS was subsequently diluted by bringing sample volume to 1 mL with lysis buffer 1. After centrifugation (20 min, 4 °C, 20,817 \times g), lysates were incubated with 6 μ L GFP_Trapping_A beads (Chromotek) overnight at 4 °C. Beads were washed four times with lysis buffer. All liquid was removed prior to the addition of sample loading buffer (containing 10mM DTT). Proteins were denatured by heating at 95 °C for 15 min and whole cell lysates with sample loading buffer containing 20 mM DTT were boiled at 95°C for 10 min. Samples were subjected to 8% SDS-PAGE, and detected by Western blotting, as indicated.

2.11 Confocal microscopy

HeLa cells were seeded to 24-well plates containing glass coverslips (Menzel Gläser, Cat# MENZCB00130RAC). SNX3-GFP and its mutant constructs were transfected to different wells. Next day, cells were washed with Phosphate Buffered Saline (PBS) and fixed with 3.7% paraformaldehyde (acid-free, Merck Millipore) in PBS for 20 min. Cells were washed with PBS for three times and treated with 0.1% Triton X-100 (Sigma-Aldrich, cat# T8787) in PBS for 10 min for permeabilization. After two times washing with PBS, blocking was performed with 5% (w/v) skim milk powder (Oxiod, cat# LP0031) in PBS for 30 min. Primary antibody incubation was done for 1 hour at room temperature with blocking buffer containing appropriate primary antibodies (Table 2.4). Cells were washed 5 min with PBS for 3 times. Secondary antibody incubation was done with the appropriate secondary anti-rabbit/mouse/rat Alexa-dye-coupled antibodies (Invitrogen) in blocking buffer for 30 min. After washing three times for 5 min, ProLong Gold antifade Mounting medium with DAPI (Life Technologies, Cat# P36941) was used for mounting of cells. Leica SP5 or SP8 microscopes equipped with appropriate solid-state lasers, HCX PL 63 times magnification oil emersion objectives and HyD detectors were used for imaging of the cells. Data were collected using a digital zoom in the range of 1.5–2.5 in 1024 by 1024 scanning format with line averaging. Post-collection image processing and colocalization analyses were performed using the ImageJ software. Colocalization was reported as Mander's overlap and Pierson's correlation coefficient, as indicated.

Table 2.4 Primary antibodies used in confocal microscopy.

Protein name	Source	Catalog number and brand	Dilution
EEA1	mouse	610457, BD	1:100
VPS26	rabbit	ab181352, Abcam	1:100
LAMP1	mouse	sc-20011, SCB	1:100
GM130	mouse	610823, BD	1:100

Golgin97	mouse	ab169287, Abcam	1:100
VAPA	rabbit	15275-1-AP, ProteinTech	1:100
RAB5	rabbit	3547, CST	1:100

SCB: SantaCruz Biotechnology, CST: Cell Signaling Technology. All these antibodies were used in Ovaa Lab.

2.12 TCF/LEF reporter assay

150000 MDA-MB-231 cells were seeded to 24-well plate. Next day, 50 nM of SNX3 and NT siRNAs were transfected to cells. 48 hours later, constructs of Signal TCF/LEF Reporter Assay Kit (LUC) (Qiagen, Cat #: CCS-018L) (250 ng) were transfected to cells. After 24 hours, Dual Luciferase® Reporter Assay System (Promega) was used according to the manufacturer's instructions. Dual-luciferase activities were measured using the Modulus Microplate Luminometer (Turner Biosystems).

CHAPTER 3

RESULTS AND DISCUSSION

3.1 Silencing of SNX3

In our previous studies, SNX3 was identified as a 3'UTR shortened-gene in TNBC patients. To investigate the role of SNX3, we firstly aimed to silence it in a TNBC cell line MDA-MB-231 to observe the effects of its absence. Initially, we tried to generate a SNX3-deleted cell model using the CRISPR/Cas9 technology. However, cells did not survive complete loss of SNX3. To overcome this obstacle, SNX3 was also knocked down with siRNA, shRNA and inducible shRNA vector.

pSUPER retro-neo.GFP containing NT (non-targetting) shRNA and SNX3 shRNA were transfected into MDA-MB-231 cells. After antibiotic selection, monoclonal cells were selected for both NT and SNX3 shRNA transfected cells. The extent of SNX3 silencing was controlled at the protein level by Western blotting (Figure 3.1).

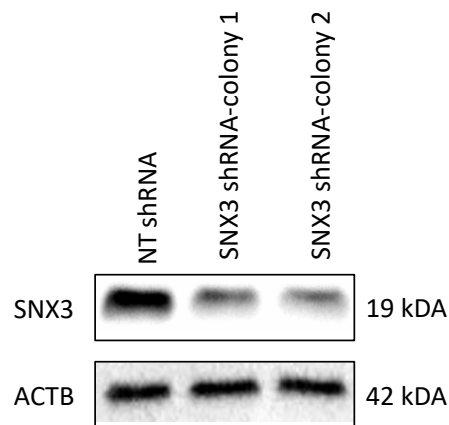


Figure 3. 1 SNX3 levels in stably transfected MDA-MB-231 cells. 50 µg protein was loaded to 10% gel. Rabbit anti-SNX3 (Proteintech, Cat #: 10772-1-AP): 1:500 dilution in 0.1% TBST with 5% BSA. Mouse anti-ACTB (SantaCruz, Cat#: SC-47778): 1:4000 dilution in 0.1% TBS-T with 3% BSA. ACTB was used as a loading control.

For the inducible silencing of SNX3, MDA-MB-231 cells were stably transfected with pcDNA6/TR to express tetracycline repressor (TetR). TetR blocks the transcription of shRNA when there is no tetracycline in the culture media. When tetracycline is used, TetR binds to tetracycline, so transcription occurs. After antibiotic selection, RNA was isolated from transfected cells, and the expression of TetR was determined with RT-PCR (Figure 3.2).

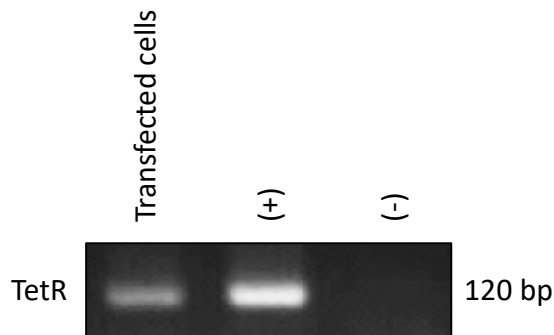


Figure 3. 2 The expression of TetR in pcDNA6/TR transfected MDA-MB-231 cells. Primers targeting TetR were used. (+) is the pcDNA6/TR vector used as the positive control. (-) indicates no template control.

pSUPERIOR-NT shRNA and pSUPERIOR-SNX3 shRNA vectors were transfected to these TetR-expressing MDA-MB-231 cells. After antibiotic selection, tetracycline induction was performed to determine the SNX3-silenced point (Figure 3.3).

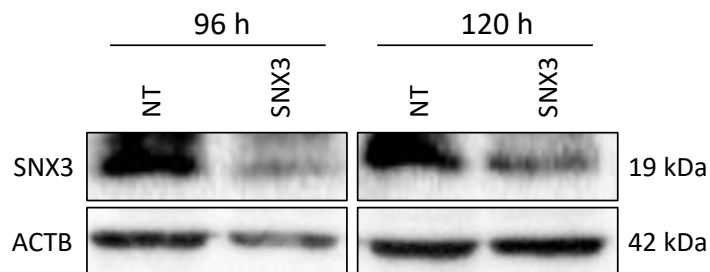


Figure 3. 3 SNX3 levels in shRNA transfected MDA-MB-231 cells. 1 μ g/ml tetracycline was given to cells in the indicated times. 50 μ g protein was loaded to 10% gel. Rabbit anti-SNX3 (Proteintech, Cat #: 10772-1-AP): 1:500 dilution in 0.1% TBST with 5% BSA. Mouse anti-ACTB (SantaCruz, Cat#: SC-47778): 1:4000 dilution in 0.1% TBS-T with 3%BSA. ACTB was used as a loading control.

Next, I tested the efficacy of siRNA (Dharmacon, Cat #: M-011521-01) for SNX3 silencing. Different concentrations of siRNA were transfected into MDA-MB-231 cells and protein expression level of SNX3 was determined (Figure 3.4)

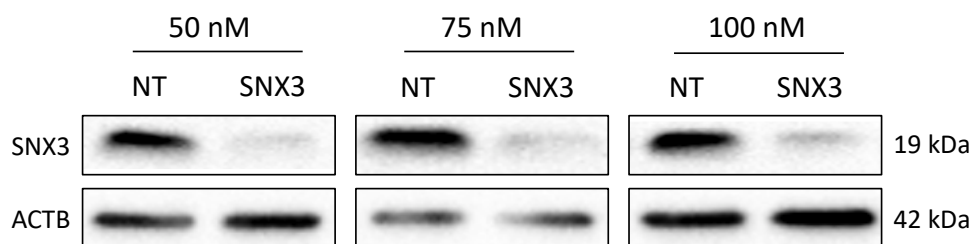


Figure 3. 4 Western blot analysis of SNX3 expression in non-target siRNA and SNX3 siRNA transfected MDA-MB-231 cells. siRNA was transfected using Dharmafect (T-2004, Dharmacon), and lysates were collected at 72 h after transfection. 50 μ g protein was loaded to 10% gel. Rabbit anti-SNX3 (Proteintech, Cat #: 10772-1-AP): 1:500 dilution in 0.1% TBST with 5% BSA. Mouse anti-ACTB (SantaCruz, Cat#: SC-47778): 1:4000 dilution in 0.1% TBS-T with 3%BSA. ACTB was used as a loading control.

According to these results, 50 nM siRNA was sufficient to silence SNX3. The rest of the siRNA transfections were done with this concentration of siRNA.

Next we investigated what happens to cells in terms of known and potential cargo receptors recognized by SNX3. The first cargo receptor tested was WLS that has been well established as a target for SNX3.^{45,46} The next candidate we investigated was EGFR, an important RTK in breast cancers, that may be regulated by SNX3.

3.2 The effect of SNX3 silencing on WLS and the Wnt pathway

TNBCs are a subtype of breast cancer that has been implicated to have active Wnt/ β -catenin pathway.¹¹¹ Therefore, we wanted to test whether SNX3 has any roles in the regulation of WLS in breast cancers and consequently in the WNT pathway.

First, we determined the level of WLS in stably SNX3-silenced (inducible) MDA-MB-231 cells (Figure 3.5). WLS levels were decreased in SNX3-silenced MDA-MB-231 cells compared to NT shRNA-expressing cells.

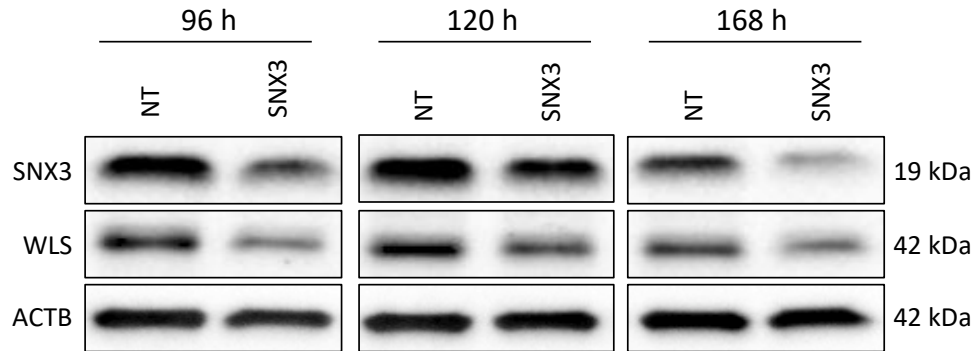


Figure 3. 5 The effect of SNX3 silencing on WLS in MDA-MB-231 cells using a tetracycline-induced system. Stably transfected MDA-MB-231 cells were induced using 1 μ g/ml tetracycline for the indicated time points. Western blot analysis was performed. 50 μ g protein was loaded to 10% gel. Rabbit anti-SNX3 (Proteintech, Cat #: 10772-1-AP): 1:500 dilution in 0.1% TBST with 5% BSA. Mouse anti-WLS (BioLegend, Cat#: 655902): 1:500 dilution in 0.1%TBS-T with 5% skim milk. Mouse anti-ACTB (SantaCruz, Cat#: SC-47778): 1:4000 dilution in 0.1% TBS-T with 3%BSA. ACTB was used as a loading control.

The effect of SNX3 silencing was also investigated in another TNBC cell line MDA-MB-468 and non-tumorigenic cell lines MCF10A and HEK293 (Figure 3.6). After 72 hours of siRNA transfection, the decrease in WLS levels was observed in MDA-MB-231, MDA-MB-468 and MCF10A cells.

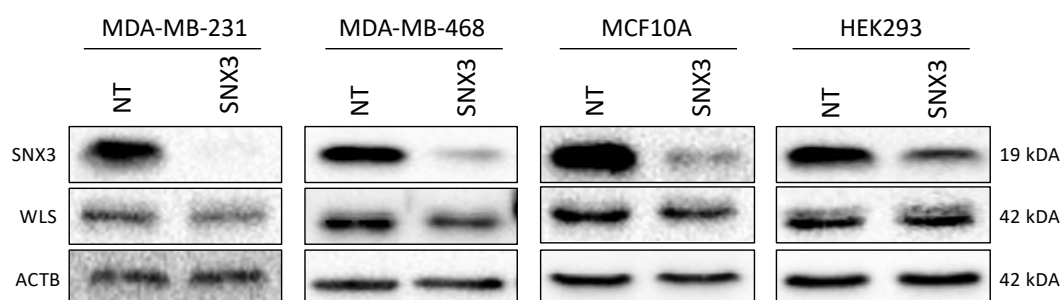


Figure 3. 6 Western blot analysis of SNX3 and WLS expressions in non-target siRNA and SNX3 siRNA transfected-cells. 50 nM siRNA was transfected using Dharmafect (T-2004, Dharmacon), and lysates were collected at 72 h after transfection. 50 μ g protein was loaded to 10% gel. Rabbit anti-SNX3 (Proteintech, Cat #: 10772-1-AP): 1:500 dilution in 0.1% TBST with 5% BSA. Mouse anti-WLS (BioLegend, Cat#: 655902): 1:500 dilution in 0.1%TBS-T with 5% skim milk. Mouse anti-ACTB (SantaCruz, Cat#: SC-47778): 1:4000 dilution in 0.1% TBS-T with 3%BSA. ACTB was used as a loading control.

Next, to investigate the effect of SNX3 silencing on the Wnt signaling pathway, we used a reporter system to test the activity of canonical Wnt pathway. In this system, several TCF/LEF responsive elements were placed upstream of Luciferase. Since TCF/LEF transcription factors are active when β -catenin goes to nucleus⁴⁹, we hypothesized that decreased β -catenin level may result in decreased TCF/LEF activity. To test this, MDA-MB-231 cells were transfected with NT and SNX3 siRNAs. After 48 hours, TCF/LEF reporter vectors and control vectors were transfected to cells. 24 hours later, dual-luciferase assay was performed (Figure 3.7).

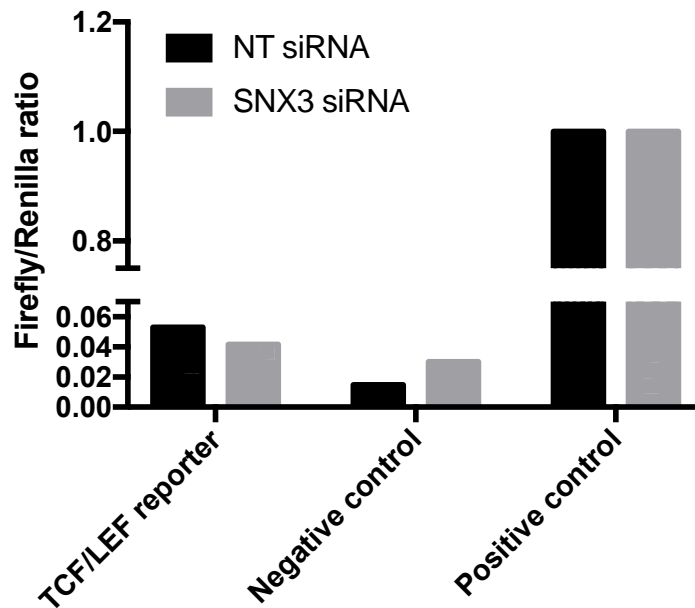


Figure 3. 7 TCF/LEF reporter assay in SNX3-silenced MDA-MB-231 cells. Cells were transfected with siRNAs for 72 hours and reporter vectors for 24 hours. In negative control, luciferase vector does not have responsive elements and any other promoter. In positive control, luciferase vector has CMV promoter, producing luciferase constitutively. The baseline in positive control samples was set to 1.

We did not detect any significant change in canonical Wnt signaling although decreased expression of WLS was observed in MDA-MB-231 cells. It is possible that these cells are not dependent enough on canonical Wnt signaling to alter Wnt dependent gene expression. It is also possible that non-canonical wnt pathway may be affected from decreased WLS levels, hence we performed a high throughput expression analysis for both canonical and non-canonical Wnt target mRNAs using Nanostring technology.

MCF10A and MDA-MB-231 cells were transfected with NT and SNX3 siRNA for 72 hours. Then, RNAs were isolated and loaded to Nanostring cartridge to be hybridized to nCounter® Vantage 3D™ Wnt Pathways Panel.

The results are shown as altered transcripts in SNX3 silenced or control cells (Figure 3.8). Interestingly, the β -catenin mRNA level decreased by 30% in SNX3 silenced

cells compared to control cells. However, there was no change in MDA-MB-231 cells. Most of WNT pathway related transcripts were down-regulated in SNX3-silenced MCF10A cells compared with the control cells, but this effect was not observed in MDA-MB-231 cells (Figure 3.8).

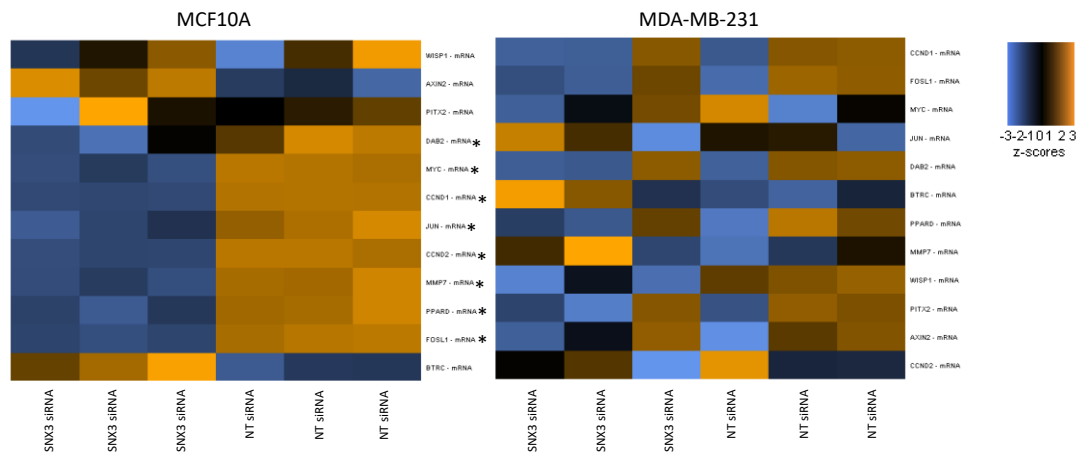


Figure 3. 8 Heatmaps showing the expression of Wnt target genes in MCF10A and MDA-MB-231 cells. 72 hours-SNX3 silenced cells were loaded to Nanostring Wnt pathway-specific cartridge. Blue and orange colors represent low and high expressions, respectively. The asterisks indicate statistical significance.

The decrease in Wnt target genes in SNX3-knockdown MCF10A cells might be due to the down-regulated β -catenin protein. To verify it, total, cytoplasmic and nuclear lysates were obtained from 72 hours SNX3-silenced MCF10A cells. β -catenin expression was detected by Western blotting (Figure 3.9).

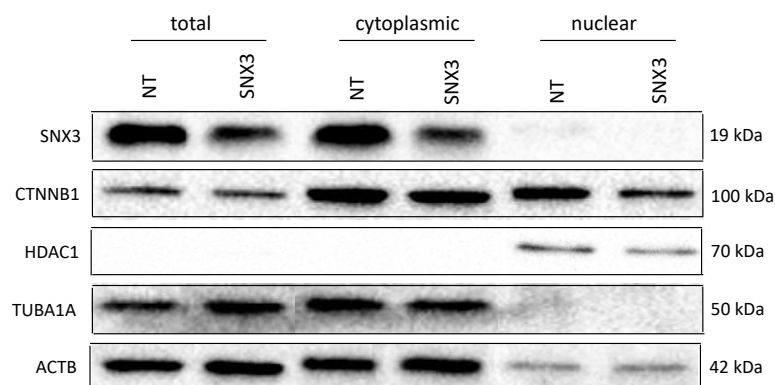


Figure 3. 9 Western blot analysis of SNX3 and CTNNB1 expressions in non-target siRNA and SNX3 siRNA transfected-cells. 50 nM siRNA was transfected using Dharmafect (T-2004, Dharmacon), and lysates were collected at 72 h after transfection. 50 µg protein was loaded to 10% gel. Rabbit anti-SNX3 (Proteintech, Cat #: 10772-1-AP): 1:500 dilution in 0.1% TBST with 5% BSA. Mouse anti-CTNNB1 (SantaCruz, Cat#: SC-133240): 1:500 dilution in 0.1%TBS-T with 5% skim milk. Mouse anti-HDAC1 (SantaCruz, Cat#: SC-81598): 1:1000 dilution in 0.1%TBS-T with 5% skim milk. Mouse anti-TUBA1A (ProteinTech, Cat#: HRP-66031): 1:5000 dilution in 0.1%TBS-T with 5% skim milk. Mouse anti-ACTB (SantaCruz, Cat#: SC-47778): 1:4000 dilution in 0.1% TBS-T with 3%BSA. HDAC1, TUBA1A, and ACTB were used as loading controls for nuclear, cytoplasmic, and total proteins, respectively.

Our results suggested that although WLS was expressed and affected from loss of SNX3, our model MDA-MB-231cells (or possibly other breast cancers) may not be very dependent on WNT signaling pathway. Although non-canonical components did change in MCF10A cells, these results will have to be further investigated.

Because SNX3 deleted cells did not survive and we did not see major effects in the Wnt pathway, we turned to the other potential SNX3 cargo, EGFR.

3.3 The effect of SNX3 silencing on the EGFR pathway

We observed that EGFR levels were decreased in 72 hours-siRNA transfected cells (Figure 3.10).

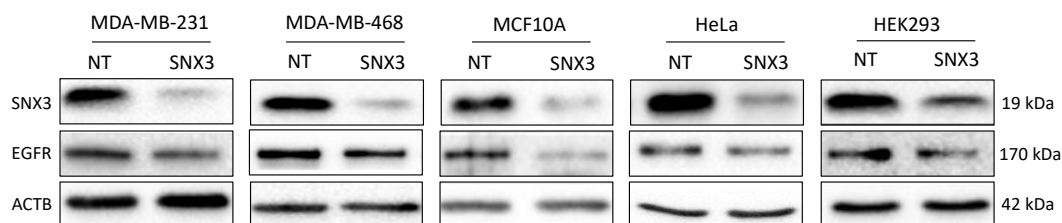


Figure 3. 10 Western blot analysis of SNX3 and EGFR expressions in non-target siRNA and SNX3 siRNA transfection different cells. 50 nM siRNA was transfected using Dharmafect (T-2004, Dharmacon), and lysates were collected at 72 h after transfection. 50 μ g protein was loaded to 10% gel. Rabbit anti-SNX3 (Proteintech, Cat #: 10772-1-AP): 1:500 dilution in 0.1% TBST with 5% BSA. Mouse anti-EGFR (SantaCruz, Cat#: SC-373746): 1:500 dilution in 0.1% TBS-T with 5% skim milk. Mouse anti-ACTB (SantaCruz, Cat#: SC-47778): 1:4000 dilution in 0.1% TBS-T with 3% BSA. ACTB was used as a loading control.

To begin investigating the impact of the EGFR level decrease, the levels of downstream components of EGFR pathways were determined (Figure 3.11). EGFR signaling starts with the binding of EGF to EGFR monomer. This binding initiates the dimerization process of EGFR, constituting EGFR homodimer. This new structure can auto-phosphorylate each other due to their kinase domains. The phosphorylation of EGFR itself results in signaling of many cascades, such as Phospholipase C gamma 1 (PLC γ 1), AKT serine/threonine kinase (AKT) and Extracellular signal-regulated kinase (ERK) pathways.¹¹² We observed that with SNX3 silencing, phosphorylation of EGFR was decreased in both cell lines. In addition, downstream pathways were also affected, meaning that phosphorylation statuses of ERK1/2 and PLC γ 1 were also downregulated. We did not observe any change in phosphorylated AKT. Due to the complexity of cancer-related pathways in cancer cells, the AKT pathway may be regulated by other factors that can inhibit the downregulation of AKT phosphorylation with SNX3 silencing.

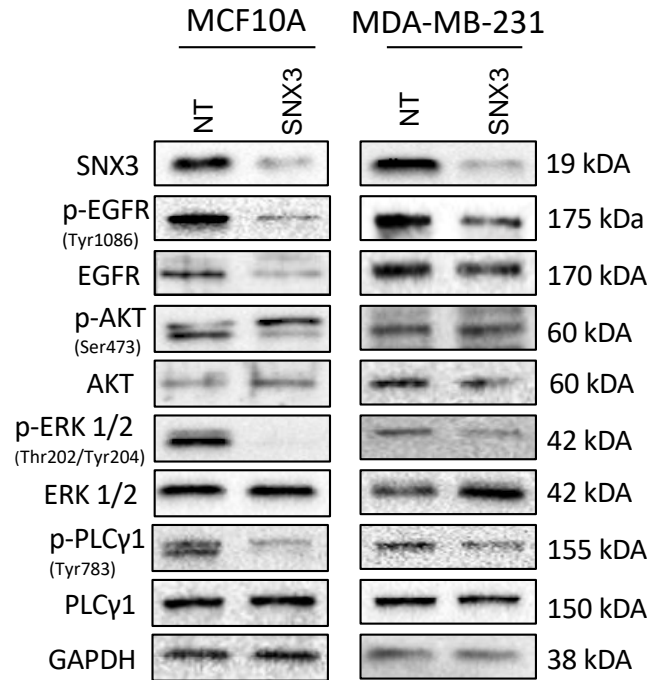


Figure 3. 11 Protein levels of EGFR signaling pathway components in MCF10A and MDA-MB-231 cells. After 72 hours of siRNA transfection, cells were collected. 50 µg protein was loaded to 10% gel. Rabbit anti-SNX3 (Proteintech, Cat #: 10772-1-AP): 1:500 dilution in 0.1% TBST with 5% BSA. Mouse anti-EGFR (SantaCruz, Cat#: SC-373746): 1:500 dilution in 0.1%TBS-T with 5% skim milk. Rabbit anti p-EGFR (Cell Signaling Technology, Cat #: 2220): 1:500 dilution in 0.1% TBST with 5% BSA. Rabbit anti p-PLCγ (Cell Signaling Technology, Cat #: 14008): 1:1000 dilution in 0.1% TBST with 5% skim milk. Rabbit anti PLCγ (Cell Signaling Technology, Cat #: 5690): 1:500 dilution in 0.1% TBST with 5% BSA. Rabbit anti p-AKT (Cell Signaling Technology, Cat #: 4060, 1:1000 dilution was prepared in 0.1 %TBS-T with 5% BSA. Rabbit anti AKT (SantaCruz, Cat #: sc-8312): 1:500 dilution in 0.1% TBS-T with 5% Skim milk. Rabbit anti p-ERK 1/2 (SantaCruz, Cat #: sc-16982): 1:500 dilution in 0.1% TBS-T with 5% skim milk. Mouse anti ERK 1/2 (SantaCruz, sc-514312): 1:200 dilution in 0.1%TBS-T with 5% BSA. Rabbit anti-GAPDH (SantaCruz, Cat #: sc-25778): 1:4000 in 0.1% TBS-T with 5% skim milk. GAPDH was used as the loading control.

It was clear that activation of EGFR pathway was significantly affected by decreased expression of SNX3. To complement the immunoblot panel we performed, we used Nanostring technology to understand the transcriptional alterations in cancer related mRNAs. We used nCounter® Vantage 3D™ Wnt Pathways Panel with SNX-

silenced cells. In this panel, there are 96 Wnt pathway-related genes. EGFR is one of the genes involved in this panel. One very interesting outcome was that, among all decreased transcripts including C-MYC, EGFR transcript levels were upregulated in SNX3 silenced cells where EGFR protein is significantly down regulated. To further confirm this result, RNAs used in Nanostring analysis were used to synthesize cDNA and RT-qPCR was performed to validate the increase in EGFR mRNA transcript levels. (Figure 3.12). Since the EGFR signaling pathway is one of the crucial pathways for motility and survival, this increase may be a response of the SNX3 silenced cells to rescue the decreased EGFR protein levels.

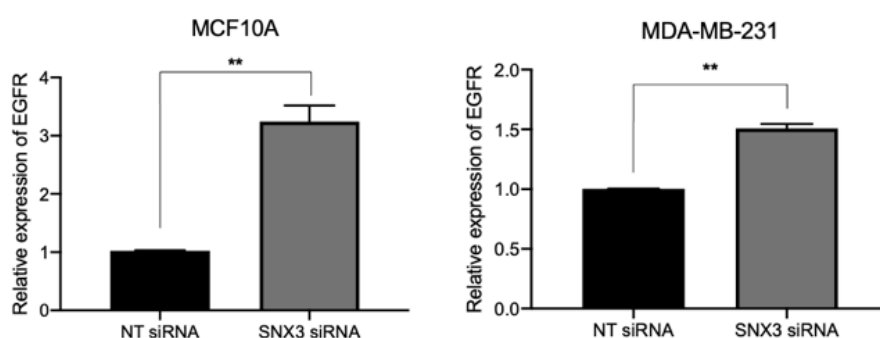


Figure 3. 12 Relative quantification of EGFR in NT and SNX3 siRNA transfected cells. 50 nM siRNA was transfected using Dharmafect (T-2004, Dharmacon), and cells were collected at 72 h after transfection. The fold change for the isoforms was normalized against the reference gene; RPLP0. Quantification was done using the reaction efficiency correction and $\Delta\Delta C_q$ method.¹⁰⁸ The baseline in NT siRNA samples was set to 1. Asterisks (**) indicate statistical significance according to the t-test.

To better understand this response, we tried to develop long term silencing of SNX3 in breast cells. First, longer-term inducible silencing of SNX3 was performed. EGFR protein levels were decreased up to 120 hours of SNX3 silencing, but increased in later time points (Figure 3.13).

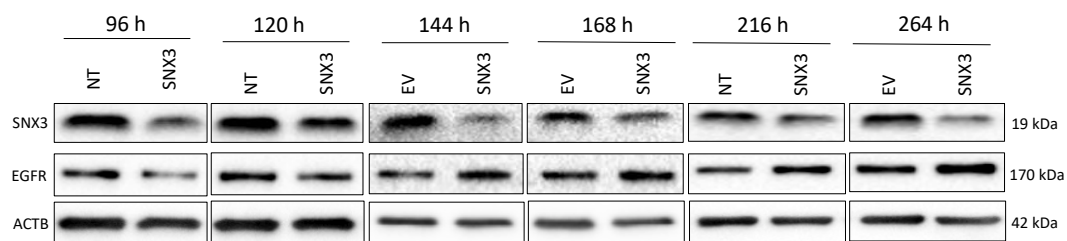


Figure 3. 13 The effect of SNX3 silencing on EGFR in MDA-MB-231 cells using a tetracycline-induced system. Stably transfected MDA-MB-231 cells were induced using 1 μ g/ml tetracycline for the indicated time points. Western blot analysis was performed. 50 μ g protein was loaded to 10% gel. Rabbit anti-SNX3 (Proteintech, Cat #: 10772-1-AP): 1:500 dilution in 0.1% TBST with 5% BSA. Mouse anti-EGFR (SantaCruz, Cat#: SC-373746): 1:500 dilution in 0.1% TBS-T with 5% skim milk. Mouse anti-ACTB (SantaCruz, Cat#: SC-47778): 1:4000 dilution in 0.1% TBS-T with 3% BSA. ACTB was used as a loading control.

The increase in EGFR levels was also observed in stably silenced cells that survived. In both MDA-MB-231 (Figure 3.14A and Figure 3.14.B) and HeLa (Figure 3.13C and 3.13D), EGFR levels were decreased in SNX3 silenced cells compared to NT shRNA transfected cells in early passages of stable cells. However, in later passages of these cells, we were surprised to see recovered and even increased levels of EGFR.

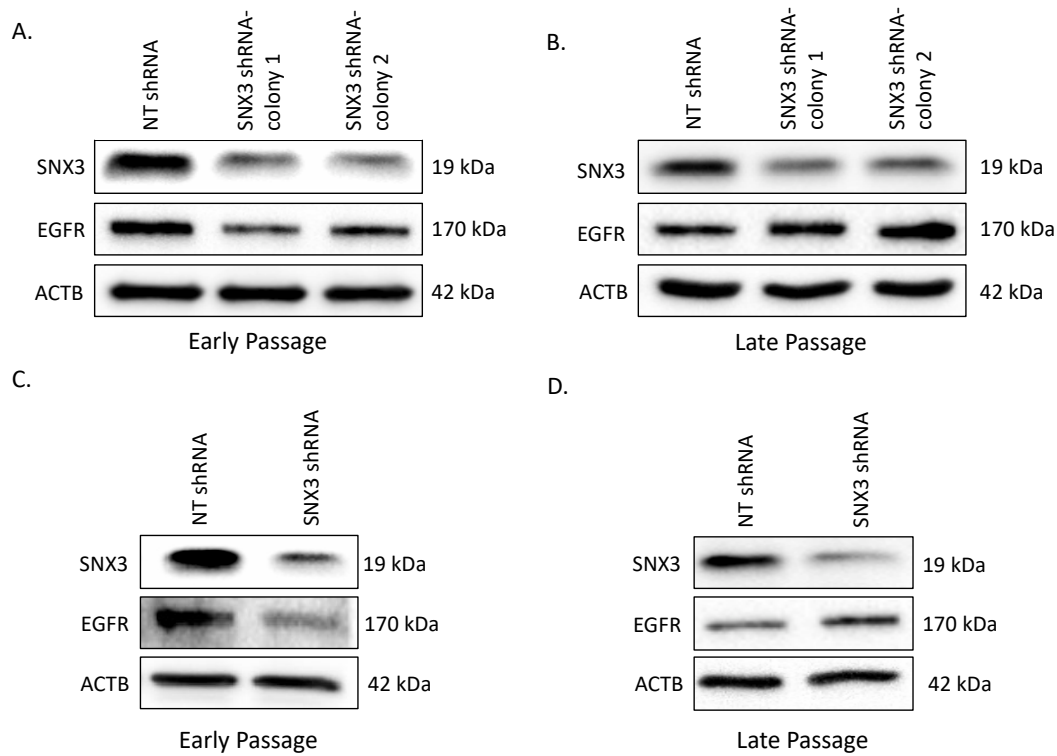


Figure 3. 14 Western blot analysis of SNX3 and EGFR expressions of stably NT and SNX3 shRNA transfected MDA-MB-231 and HeLa cells. A. Early effect of SNX3 silencing. Cells were collected after the generation of the stable cell line. B. Late effect of SNX3 silencing. Cells were collected after several passages. 50 μ g protein was loaded to 10% gel. Rabbit anti-SNX3 (Proteintech, Cat #: 10772-1-AP): 1:500 dilution in 0.1% TBST with 5% BSA. Mouse anti-EGFR (SantaCruz, Cat#: SC-373746): 1:500 dilution in 0.1%TBS-T with 5% skim milk. Mouse anti-ACTB (SantaCruz, Cat#: SC-47778): 1:4000 dilution in 0.1% TBS-T with 3%BSA. ACTB was used as a loading control.

To sum up, the short-term knockdown of SNX3 led to decreased EGFR protein levels and increased EGFR mRNA levels compared to controls. However, prolonged SNX3 silencing resulted in increased EGFR protein levels.

3.4 The interaction of SNX3 and EGFR

Proximity-based labeling (TurboID) was used to test whether SNX3 and EGFR interact. The principle of this technique is that proteins come to close proximity are biotinylated with the enzyme BirA fused to SNX3. We used “TurboID”, which is the evolved version of the “BirA” biotin ligase enzyme, having fast tagging kinetics than BirA.¹¹³ SNX3 coding sequence was cloned N-terminus of TurboID into the pcDNA 3.1 (-) vector. HA-tag was also added to C-terminus of TurboID. For control, only TurboID-HA was cloned into the pcDNA 3.1 (-) vector. We used two different cell models to test the activity of SNX3-TurboID-HA construct: HEK293 and HeLa cells. They were treated with 50 μ M final concentration of biotin for 2 and 4 hours.

First, HEK293 cells were separately transfected with TurboID-HA and SNX3-TurboID-HA vectors. EGFR-GFP vector was also co-transfected to cells with TurboID vectors. After 4 hours of biotinylation, cells were collected and lysates were incubated with neutravidin beads to pull-down biotinylated proteins.

In Figure 3.15, two western blots are shown. The left image shows the result of immunoprecipitated (IP) lysates. Anti-HA antibody was used to detect biotinylated SNX3 proteins. Anti-GFP antibody was used to detect the biotinylated GFP-tagged EGFR proteins if EGFR comes to close proximity to SNX3. The image on the right shows the whole cell lysates (without neutravidin pull-down) to specify equal loading of proteins. As a result, EGFR was biotinylated in SNX3-TurboID-HA transfected cells.

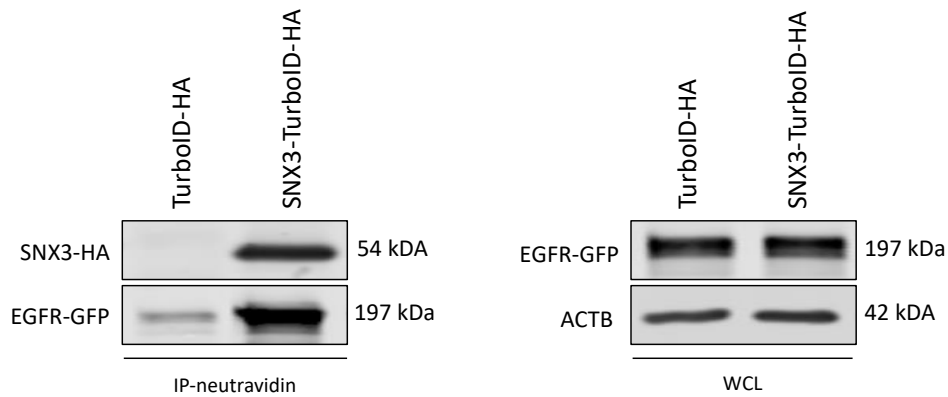


Figure 3. 15 Biotinylation of SNX3 and its interactants. Proximity-based labeling with biotin and TurboID was used to tag the proteins near SNX3 in HEK293 cells. SNX3-TurboID-HA and EGFR-GFP vectors were co-transfected to cells. Biotinylated proteins were pulled-down with neutravidin beads (Thermo Scientific, Cat# 29202). Rabbit anti-EGFR (Millipore, Cat # 06-847): 1:1000 dilution in 0.1%TBS-T with 5% skim milk. Rabbit anti-mGFP (REF 61): 1:1000 dilution in 0.1%TBS-T with 5% skim milk. Mouse anti-HA (HA.11 (16B12) (Covance, Cat# MMS-101R): 1:1000 dilution in 0.1%TBS-T with 5% skim milk. Mouse anti- β -actin (Sigma-Aldrich, Cat# A5441): was used as a loading control in a 1:10,000 dilution in 0.1%TBS-T with 5% skim milk. Whole-cell lysate (WCL) was used to show the equal loading of proteins.

The fact that SNX3 and EGFR were in close proximity, we wanted to test this interaction in a dynamic set-up of EGF treatment. The low or high concentration of EGF directs EGFR to recycle back to PM or degradation by the lysosome, respectively. To delineate which path SNX3 and EGFR interact, cells were treated with low EGF (5 ng/ml) or with high (25 ng/ml) EGF and proximity-based labeling assay was applied. With high EGF concentration, SNX3-TurboID biotinylation of EGFR was lower as early as 15 minutes. Conversely, with low EGF dose, biotinylation of EGFR was highest at 15 and 30 minutes of EGF stimulation (Figure 3.16).

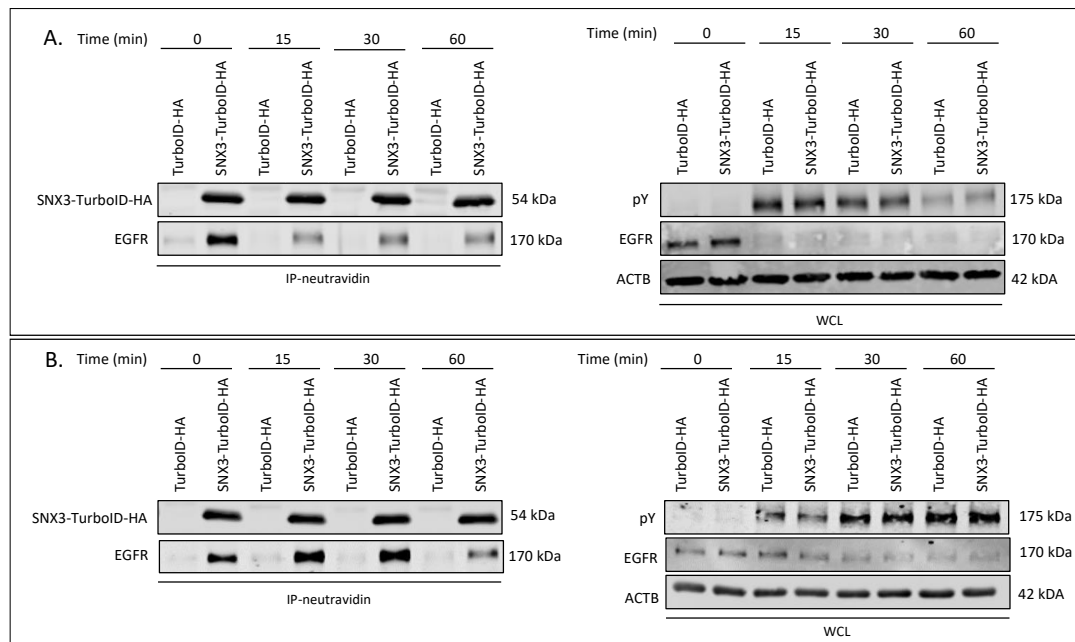


Figure 3.16 Biotinylation of SNX3 and its interactions with EGFR after EGF treatment. Proximity-based labeling with biotin and TurboID was used to tag the proteins near SNX3 in HeLa cells. SNX3-TurboID-HA and EGFR-GFP vectors were co-transfected to cells. 24 h later, A. 25 ng/ml EGF and B. 5 ng/ml EGF were added. Biotinylated proteins were pulled-down with neutravidin beads (Thermo Scientific, Cat# 29202). Mouse anti-phosphotyrosine (4G10 Millipore, Cat# 05-321): 1:1000 dilution in 0.1% TBS-T with 5% skim milk. Rabbit anti-EGFR (Millipore, Cat # 06-847): 1:1000 dilution in 0.1% TBS-T with 5% skim milk. Rabbit anti-mGFP (REF 61): 1:1000 dilution in 0.1% TBS-T with 5% skim milk. Mouse anti-HA (HA.11 (16B12) (Covance, Cat# MMS-101R): 1:1000 dilution in 0.1% TBS-T with 5% skim milk. Rabbit anti-VPS26 (Abcam, Cat# ab181352): 1:1000 dilution in 0.1% TBS-T with 5% skim milk. Mouse anti- β -actin (Sigma-Aldrich, Cat# A5441): was used as a loading control in a 1:10,000 dilution in 0.1% TBS-T with 5% skim milk. Whole-cell lysate (WCL) was used to show the equal loading of proteins.

The amount of EGFR on the plasma membrane after EGF stimulation was shown with flow cytometry. 25 ng/ml of EGF treatment led to immediate loss of EGFR on the plasma membrane, whereas with 5 ng/ml of EGF, EGFR was mostly retained on the cell membrane, suggesting more recycling than lysosomal degradation at early time points (Figure 3.17).

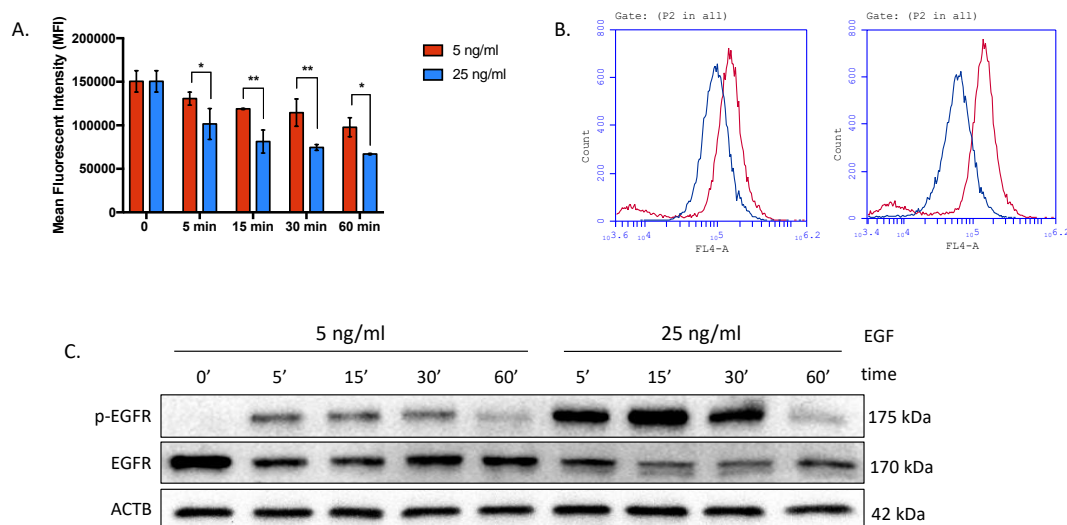


Figure 3. 17 Cell surface EGFR levels determined by flow cytometry on EGF-treated HeLa cells. A. Mean fluorescent intensity (MFI) was used to graph cell surface levels of EGFR. B. Histograms of 5 ng/ml and 25 ng/ml EGF treatment for 60 minutes were obtained from BD Accuri C6 software. The red line indicates the control sample (0 min). The blue line indicates EGF treated samples. C. The Western blotting technique was used to determine the total levels of EGFR and its phosphorylated form. Mouse anti-EGFR (SantaCruz, Cat#: SC-373746): 1:500 dilution in 0.1% TBS-T with 5% skim milk. Rabbit anti p-EGFR (Cell Signaling Technology, Cat #: 2220): 1:500 dilution in 0.1% TBST with 5% BSA. Mouse anti-ACTB (SantaCruz, Cat#: SC-47778): 1:4000 dilution in 0.1% TBS-T with 3% BSA. ACTB was used as a loading control. The asterisks indicate statistical significance according to 2-way ANOVA with Sidak's multiple comparison test.

These results showed that biotinylation of EGFR was more during 5 ng/ml of EGF treatment which did not lead to decreased surface levels of EGFR. On the contrary, high doses of EGF treatment led to decreased surface EGFR levels, suggesting less recycling. In this situation, biotinylation of EGFR was also decreasing in a time dependent manner.

To look deeper into how SNX3 may interact with EGFR in an EGF dependent manner, we hypothesized that ubiquitination (Ub) of SNX3 may have a role since Ub is known to regulate, endocytosis, and endocytic trafficking.⁷²

3.5 Ubiquitination of SNX3

Ubiquitination occurs on lysine residues of the target proteins.⁷² To assess potential Ub sites, 5 lysines were chosen according to ubiquitination site prediction tools: L61, L63, L95, L119, and L128.¹¹⁴ These sites were mutated to Arginine to block the any potential ubiquitination events. L61 and L63 were mutated together due to their close locations. All mutations were performed on the SNX3-GFP coding sequence in the pEGFP-N1 vector.

To test the ubiquitination status of these lysine residues, ubiquitination assay was carried out (Figure 3.18). HEK293 cells were transfected with HA-Ub, SNX3-GFP wild-type (WT) or its mutant forms for 24 hours. In no-Ub controls, only SNX3-GFP WT was transfected. GFP-trap beads were used to pull-down GFP proteins. Immunoprecipitated proteins and whole cell lysates were loaded to 8% SDS-polyacrylamide gel. Anti-HA antibody was used to show the ubiquitination and anti-GFP antibody indicated the GFP-tagged SNX3.

According to immunoblot results, SNX3 is ubiquitinated and mutations affect the ubiquitination of SNX3. Interestingly, the K95R mutant of SNX3 was not ubiquitinated as WT did and the K199R mutant was ubiquitinated more than WT.

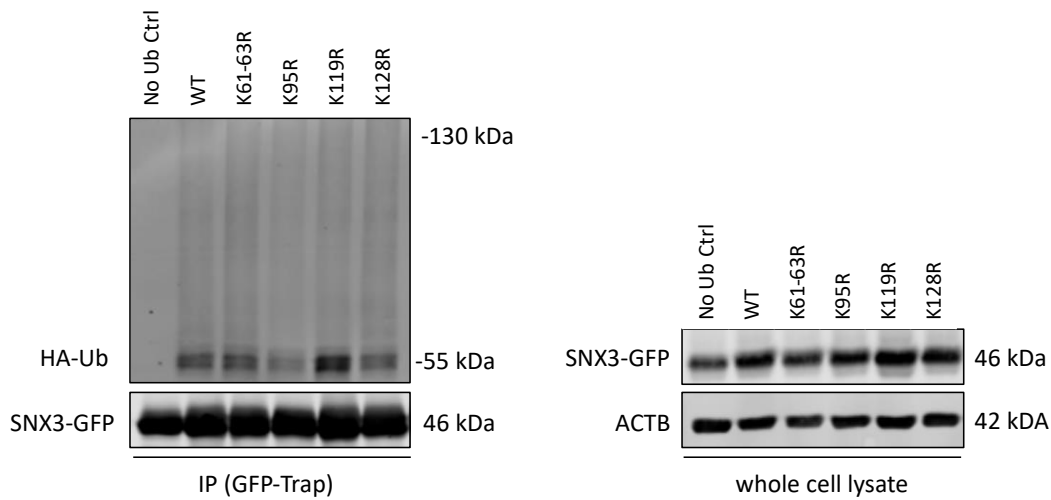


Figure 3. 18 Ubiquitination status of SNX3 and its mutated versions. HA-Ub and SNX3-GFP vectors were co-transfected to HEK293 cells. GFP-trap beads were used to pull down SNX3-GFP proteins. Rabbit anti-mGFP (REF 61): 1:1000 dilution in 0.1%TBS-T with 5% skim milk. Mouse anti-HA (HA.11 (16B12) (Covance, Cat# MMS-101R): 1:1000 dilution in 0.1%TBS-T with 5% skim milk. Mouse anti- β -actin (Sigma-Aldrich, Cat# A5441): was used as a loading control in a 1:10,000 dilution in 0.1%TBS-T with 5% skim milk. Whole-cell lysate (WCL) was used to show the equal loading of proteins.

Next, EGF was given to HEK293 cells transfected with SNX3-GFP WT to see the effect of EGF on SNX3 ubiquitination (Figure 3.19). It was observed that ubiquitination of SNX3 was increased with 30 min. of EGF treatment.

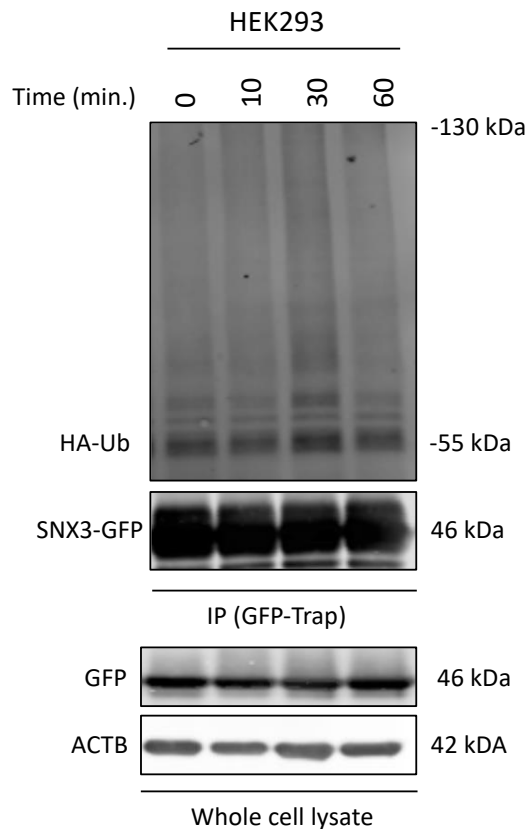


Figure 3. 19 Ubiquitination status of SNX3 with EGF treatment. HA-Ub and SNX3-GFP vectors were co-transfected to HEK293 cells. 25 ng/ml EGF was given for indicated times. GFP-trap beads were used to pull down SNX3-GFP proteins. Mouse anti-phosphotyrosine (4G10 Millipore, Cat# 05-321): 1:1000 dilution in 0.1%TBS-T with 5% skim milk. Rabbit anti-mGFP¹⁰⁹: 1:1000 dilution in 0.1%TBS-T with 5% skim milk. Mouse anti-HA (HA.11 (16B12) (Covance, Cat# MMS-101R): 1:1000 dilution in 0.1%TBS-T with 5% skim milk. Mouse anti- β -actin (Sigma-Aldrich, Cat# A5441): was used as a loading control in a 1:10,000 dilution in 0.1%TBS-T with 5% skim milk. Whole cell lysate (WCL) was used to show the equal loading of proteins.

These results suggested that EGF treatment increased the ubiquitination of SNX3. In order to further investigate SNX3 ubiquitination upon EGF treatment, we used SNX3-GFP WT along with its lysine mutant forms and treated transfected cells with EGF for 30 minutes. (Figure 3.20). EGF treatment showed slightly increased ubiquitination of WT SNX3 and its mutated forms.

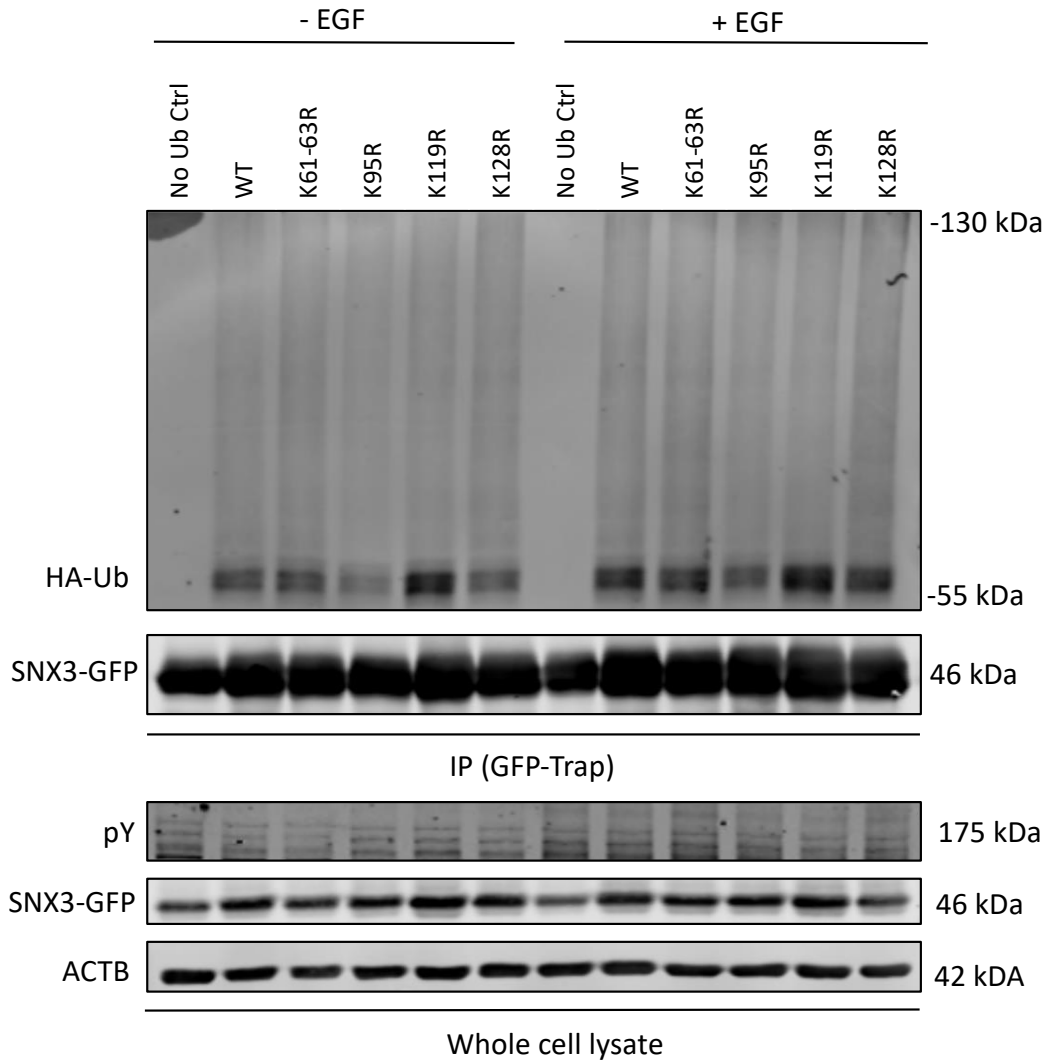


Figure 3. 20 Ubiquitination status of SNX3 and its mutated versions with EGF treatment. HA-Ub and SNX3-GFP vectors were co-transfected to HEK293 cells. 25 ng/ml EGF was given for 30 minutes. GFP-trap beads were used to pull down SNX3-GFP proteins. Mouse anti-phosphotyrosine (4G10 Millipore, Cat# 05-321): 1:1000 dilution in 0.1%TBS-T with 5% skim milk. Rabbit anti-mGFP¹⁰⁹: 1:1000 dilution in 0.1%TBS-T with 5% skim milk. Mouse anti-HA (HA.11 (16B12) (Covance, Cat# MMS-101R): 1:1000 dilution in 0.1%TBS-T with 5% skim milk. Mouse anti- β -actin (Sigma-Aldrich, Cat# A5441): was used as a loading control in a 1:10,000 dilution in 0.1%TBS-T with 5% skim milk. Whole cell lysate (WCL) was used to show the equal loading of proteins.

Given the potential ubiquitination of SNX3, the next step was observing the subcellular localization of Lysine mutant SNX3 in the cell. For this purpose, HeLa cells were transfected with SNX3-GFP mutant vectors and cells were stained with indicated markers (Figure 3.21). All the mutants were localized in early endosomes (RAB5) while K95R mutant was distributed in cytosol. This result showed that K95 could be an important site for the localization of SNX3 to early endosomes.

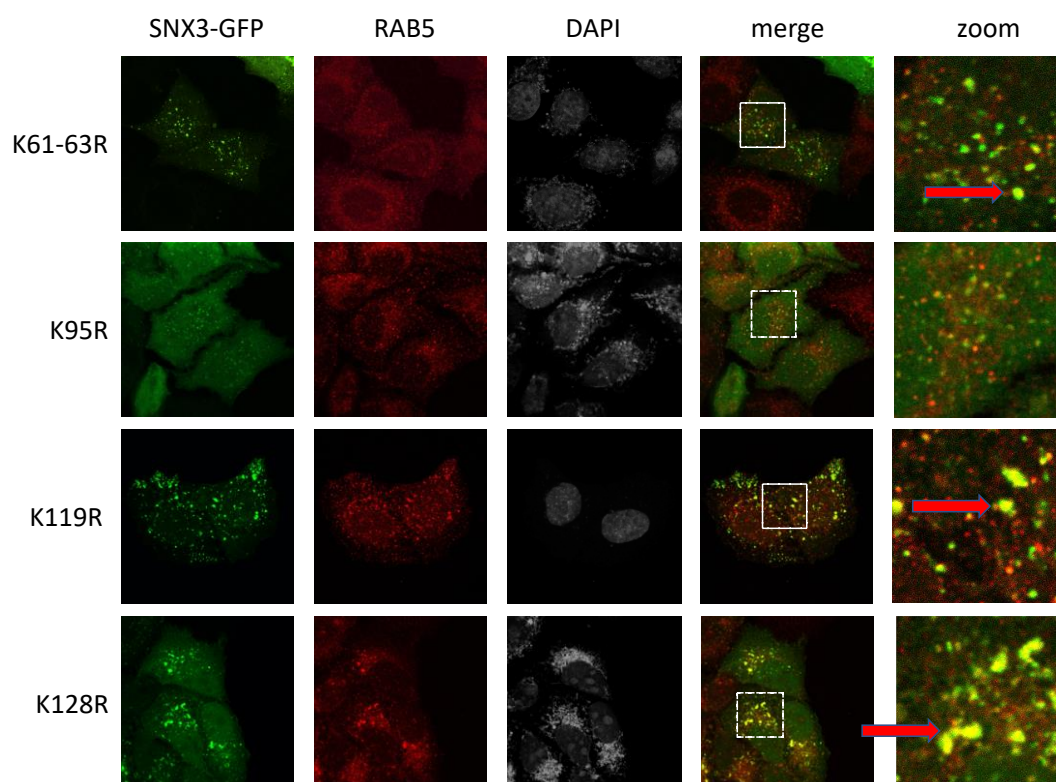


Figure 3. 21 Confocal microscopy images of SNX3-GFP WT and its mutant forms. HeLa cells were transfected with SNX3-GFP WT and other 4 mutant vectors (K61-63R, K95R, K119R and K128R). After 24 hours, cells were fixed and immunostained against indicated marker: rabbit anti-Rab5 (Cell Signaling, Cat# 3547s; 1:100). DAPI staining was performed with mounting media containing DAPI. White dashed squares in the merge images represent the zoomed area. Red arrows show the colocalization of the signals.

Our results suggested that K95 could potentially be a ubiquitinated lysine. To test whether this mutant behaves any different than WT SNX3, further co-localization experiments were performed. SNX3-GFP WT and SNX3_K95R-GFP vectors were transfected to HeLa cells. Antibodies against early and late endosomes, *cis*- and *trans*-Golgi, and Endoplasmic Reticulum markers were used to address SNX3 localization. Confocal microscopic images were statistically analyzed. SNX3 localizes in early endosomes and interacts with the retromer complex (REF). We showed that WT SNX3 indeed colocalized with EEA1 (early endosome marker) and VPS26 (a component of the retromer complex). Conversely, the K95R mutant was cytoplasmic and colocalization of this mutant with the retromer complex protein VPS26 was decreased compared to WT. Both SNX3 WT and SNX3-K95R were not found in late endosomes (LAMP1), *cis*-Golgi (GM130), *trans*-Golgi (golgin 97) and Endoplasmic Reticulum (VAPA) (Figure 3.22).

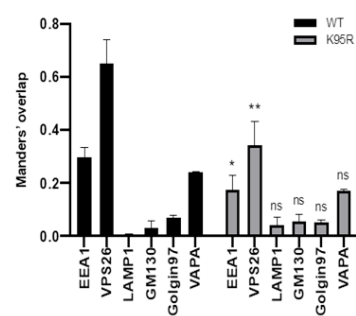
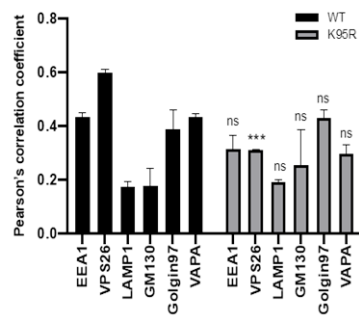
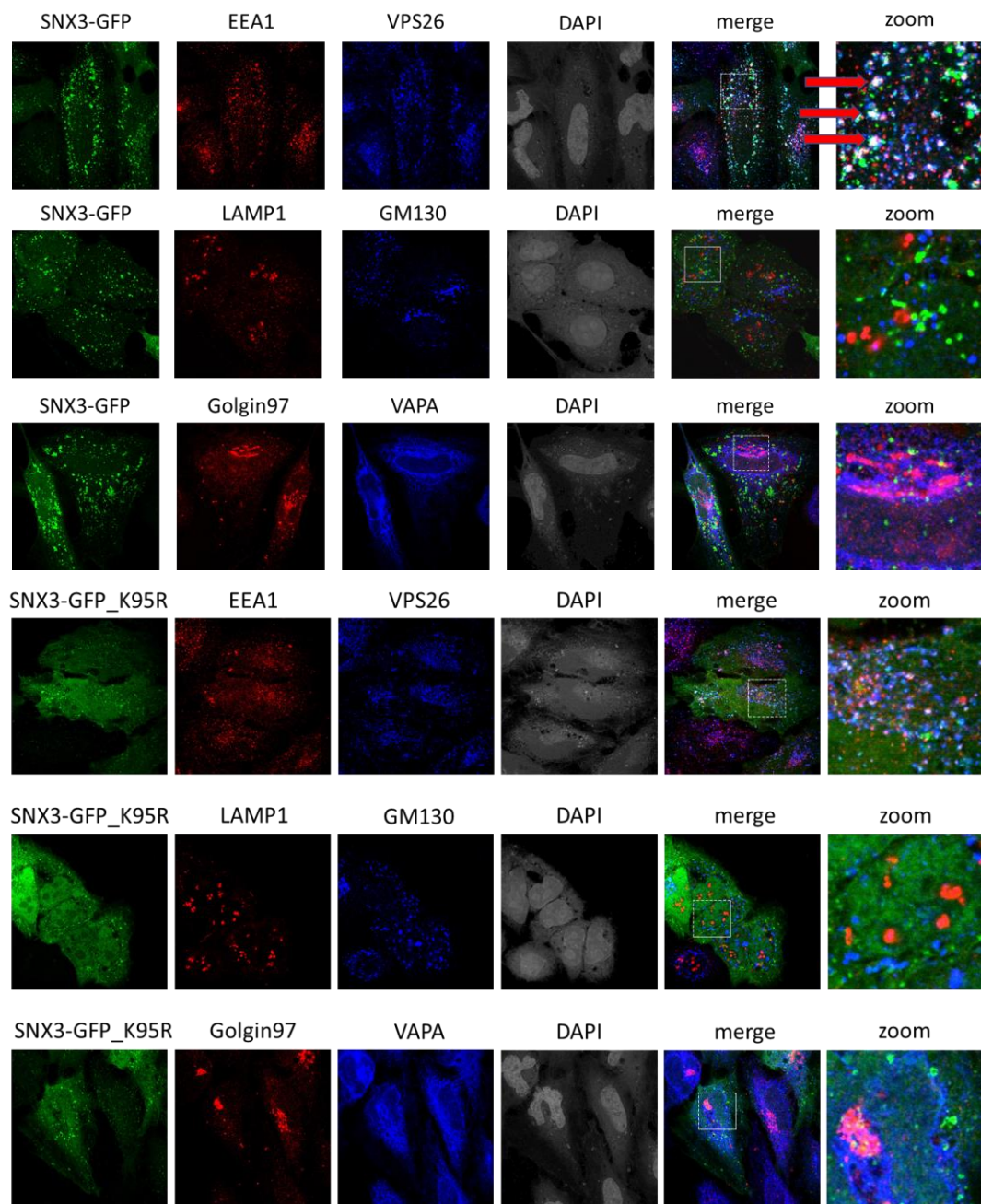


Figure 3. 22 Confocal microscopy images of SNX3-GFP WT and SNX3-GFP K95R mutant. HeLa cells were transfected with SNX3-GFP WT and SNX3-GFP K95R vectors. After 24 hours, cells were fixed and immunostained against indicated markers: mouse anti-EEA1 (BD Transduction Laboratories, Cat# 610457; 1:100), rabbit anti-VPS26 (Abcam, Cat# ab181352; 1:100), mouse anti-LAMP1 (Santa Cruz Biotechnology, Cat# sc-20011; 1:100), mouse anti-GM130 (BD, Cat#: 610823), mouse anti-Golgin97 (Abcam, Cat# ab169287; 1:100), rabbit anti-VAPA (ProteinTech, Cat# 15275-1-AP; 1:100). DAPI staining was performed with mounting media containing DAPI. White dashed squares in the merge images represent the zoomed area. Red arrows show the colocalization of the signals. Image J was used to calculate the correlation. Pearson's correlation coefficient and Manders' overlap values were used for statistics. The asterisks indicate statistical significance with the t-test.

Cytoplasmic distribution of SNX3-K95R and losing its interactions with early endosome and retromer lead us to consider the loss of interaction of SNX3-K95R mutant with its cargo proteins. To test this idea, SNX3-GFP WT and the K95R mutant were transfected to HeLa cells. After 24 hours, 25 ng/ml Alexa-fluor labelled-EGF was given for 30 min. EEA1 and LAMP1 were labeled and cells were visualized under the confocal microscope. It was observed that SNX3 WT colocalized with EGF in early endosomes, not in lysosomes; however, the K95R mutant did not localized with endocytosed EGF (Figure 3.23). This result also suggested that K95R mutant of SNX3 may not interact with internalized EGFR.

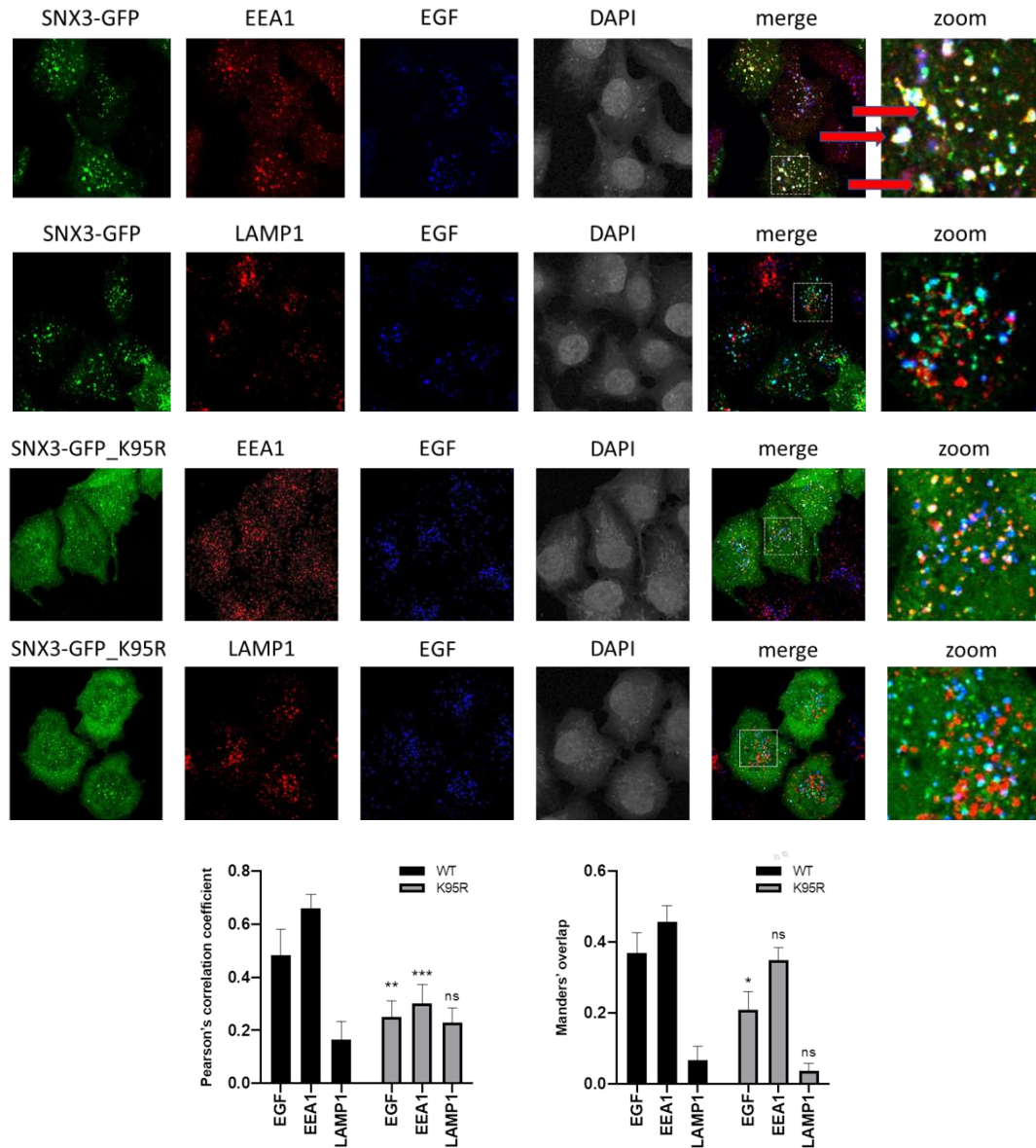


Figure 3. 23 Confocal microscopy images of EGF-treated SNX3-GFP WT and SNX3-GFP K95R mutant. HeLa cells were transfected with SNX3-GFP WT and SNX3-GFP K95R vectors. After 24 hours, cells were treated with 25 ng/ml Alexa-fluor 647 labeled EGF (Invitrogen, Cat#: E35351) for 30 min. then, they were fixed and immunostained against indicated markers: mouse anti-EEA1 (BD Transduction Laboratories, Cat# 610457; 1:100), mouse anti-LAMP1 (Santa Cruz Biotechnology, Cat# sc-20011; 1:100). DAPI staining was performed with mounting media containing DAPI. White dashed squares in the merge images represent the zoomed area. Red arrows show the colocalization of the signals. Image J was used to calculate the correlation. Pearson's correlation coefficient and Manders' overlap values were used for statistics. The asterisks indicate statistical significance with the t-test.

In addition to decreased Ub of K95R, K95 is one of the 4 residues that interact with inositol phosphate on endosomes via hydrogen bonding.⁶¹ Therefore, K95 may be a critical amino acid for SNX3 recruitment to the early endosome.

CHAPTER 4

CONCLUSION

In this study, we investigated role of SNX3 in connection with EGFR. SNX3 is a sorting protein which recruits the retromer complex to early endosomes for cargo recycling.¹¹⁵ One of the cargo proteins recycled by SNX3 retromer identified in *C. elegans* and *Drosophila* was WLS.^{45,46} WLS carries Wnt ligands from Golgi to plasma membrane for secretion.¹¹⁶ In order to investigate the function of SNX3 in breast cancer, SNX3 was silenced in several breast cancer cell lines, additionally in other non-breast cell lines, and WLS levels were determined. Both short-term and long-term silencing of SNX3 resulted in decreased WLS protein levels. To test the effect of SNX3 silencing on Wnt/ β -catenin (canonical) signaling pathway, TCF/LEF reporter assay was performed to determine the activity of this pathway in MDA-MB-231 cells. Interestingly, we did not observe any change in TCF/LEF luciferase activity. Hence, we concluded that may be the models we used were not so much dependent on Wnt secretion and hence nuclear activity of TCF/LEF factors were not affected from decreased WLS levels.

Next we turned to EGFR as another possible cargo of SNX3.¹⁰⁵ The protein level of EGFR was also decreased in SNX3 silenced breast cancer cells, in HeLa and HEK293 cells. The impact of this decrease was further investigated through the downstream components of EGFR pathway. In SNX3-silenced MCF10A and MDA-MB-231 cells, decreased levels of phosphorylated forms of EGFR, ERK1/2 and PLC γ 1 suggesting that SNX3 silencing downregulated the components of major downstream signaling pathways of EGFR signaling. Interestingly, EGFR mRNA levels in these cells were increased in SNX3-silenced cells compared to control detected by a targeted expression experiment. we reasoned that this increase may be due to an attempt to restore EGFR protein level in SNX3-silenced cells since EGFR is an important protein having roles in the survival of triple-negative breast cancer

cells.¹¹⁷ To further understand this increase, cells with long-term silencing of SNX3 were used. In early passages of stably SNX3 silenced cells, EGFR protein levels were decreased; however, they were increased in late passages. This situation may be a response of the cells to overcome the downregulation of EGFR to survive.

Next, the interaction of SNX3 and EGFR was tested using proximity-based labelling (TurboID) technique. In HEK293 cells, SNX3-TurboID biotinylated EGFR. The impact of EGF treatment was also investigated with TurboID technique. we observed that low concentration of EGF (5 ng/ml) treatment resulted with biotinylation of EGFR by SNX3-TurboID; however, with high concentration of EGF (25 ng/ml), biotinylation was lost in HeLa cells. These results are in agreement with earlier observations that the route of EGFR changes with different concentration of EGF. High dose EGF (25 ng/ml and more) leads to the degradation of EGFR, whereas low dose EGF (5 ng/ml and less) results in the recycling of EGFR to plasma membrane.⁸⁹ Therefore, the increase in SNX3-EGFR proximity with low EGF concentration may suggest that SNX3 may involve in the process of EGFR trafficking back to plasma membrane. The amount of cell surface EGFR levels after high (25 ng/ml) and low (5 ng/ml) concentration of EGF treatments were determined in HeLa cells with flow cytometry. The result also suggested that low dose EGF-treated cells had more EGFR on their cell membranes than high-dose EGF-treated cells.

SNX3 was also investigated through potential post-translational modification, ubiquitination. We tried to determine the ubiquitination site of SNX3; therefore, possible ubiquitination sites (lysine residues) were mutated on SNX3 coding sequence. Ubiquitination assay was performed using HEK293 cells. Among the mutants, K95 mutant seemed to affect the ubiquitination of SNX3 since ubiquitination was decreased on this site compared to wild-type SNX3 ubiquitination. Interestingly, ubiquitination of SNX3 was increased when K199 was mutated. This mutant may increase the level of SNX3 ubiquitination through another Lysines. More studies have to be performed to determine the ubiquitination type of on these lysine residues of SNX3. Next, the effect of EGF treatment on SNX3 ubiquitination was investigated. EGF treatment for 30 minutes increased the

ubiquitination of SNX3 in HEK293 cells compared to untreated cells. This increase in ubiquitination status of SNX3 with EGF was further investigated with mutant forms of SNX3 in HEK293 cells. Surprisingly, EGF treatment increased the ubiquitination of all wild-type SNX3 and its mutants, suggesting that EGF may enhance the overall ubiquitination of SNX3. Then, to further investigate these lysine mutants of SNX3, their subcellular localizations were determined using confocal microscopy in HeLa cells. All the other mutants, except K95R, were localized to early endosomes as SNX3 wild-type. Interestingly, K95R showed a cytoplasmic distribution in cells. our results show that K95 may be an important residue for membrane binding of SNX3. Neither WT SNX3 nor K95R mutant was localized to late endosome, Golgi or the Endoplasmic Reticulum. Cytoplasmic distribution of SNX3-K95R and losing its interactions with early endosome and retromer lead us to consider the loss of interaction of SNX3-K95R mutant with its cargo proteins. Alexa-Fluor labelled EGF was given to cells for 30 minutes to test the interaction of both WT SNX3 and K95R mutant with EGF. The result showed us that SNX3-K95R did not co-localize with EGF.

Overall, we showed that EGFR levels are modulated by SNX3 and that EGF stimulation may regulate SNX3 through ubiquitination. Given these findings, deregulated EGFR expression in a subset of tumors may be attributed to SNX3 function. These findings may have future implication for EGFR targeted therapies.

REFERENCES

1. Teasdale RD, Loci D, Houghton F, Karlsson L, Gleeson PA. A large family of endosome-localized proteins related to sorting nexin 1. *Biochem J.* 2001;358(Pt 1):7-16.
2. Cullen PJ. Endosomal sorting and signalling: an emerging role for sorting nexins. *Nat Rev Mol Cell Biol.* 2008;9(7):574-582.
3. Carlton J, Bujny M, Rutherford A, Cullen P. Sorting nexins--unifying trends and new perspectives. *Traffic.* 2005;6(2):75-82.
4. Seet LF, Hong W. The Phox (PX) domain proteins and membrane traffic. *Biochim Biophys Acta.* 2006;1761(8):878-896.
5. van Weering JR, Sessions RB, Traer CJ, et al. Molecular basis for SNX-BAR-mediated assembly of distinct endosomal sorting tubules. *Embo j.* 2012;31(23):4466-4480.
6. Zimmerberg J, McLaughlin S. Membrane curvature: how BAR domains bend bilayers. *Curr Biol.* 2004;14(6):R250-252.
7. Park J, Kim Y, Lee S, et al. SNX18 shares a redundant role with SNX9 and modulates endocytic trafficking at the plasma membrane. *J Cell Sci.* 2010;123(Pt 10):1742-1750.
8. Traer CJ, Rutherford AC, Palmer KJ, et al. SNX4 coordinates endosomal sorting of TfnR with dynein-mediated transport into the endocytic recycling compartment. *Nat Cell Biol.* 2007;9(12):1370-1380.
9. Dyve AB, Bergan J, Utskarpen A, Sandvig K. Sorting nexin 8 regulates endosome-to-Golgi transport. *Biochem Biophys Res Commun.* 2009;390(1):109-114.
10. Wassmer T, Attar N, Harterink M, et al. The retromer coat complex coordinates endosomal sorting and dynein-mediated transport, with carrier recognition by the trans-Golgi network. *Dev Cell.* 2009;17(1):110-122.
11. Chishti AH, Kim AC, Marfatia SM, et al. The FERM domain: a unique module involved in the linkage of cytoplasmic proteins to the membrane. *Trends Biochem Sci.* 1998;23(8):281-282.

12. Ghai R, Bugarcic A, Liu H, et al. Structural basis for endosomal trafficking of diverse transmembrane cargos by PX-FERM proteins. *Proc Natl Acad Sci U S A*. 2013;110(8):E643-652.
13. Burden JJ, Sun XM, Garcia AB, Soutar AK. Sorting motifs in the intracellular domain of the low density lipoprotein receptor interact with a novel domain of sorting nexin-17. *J Biol Chem*. 2004;279(16):16237-16245.
14. Stockinger W, Sailer B, Strasser V, et al. The PX-domain protein SNX17 interacts with members of the LDL receptor family and modulates endocytosis of the LDL receptor. *Embo j*. 2002;21(16):4259-4267.
15. van Kerkhof P, Lee J, McCormick L, et al. Sorting nexin 17 facilitates LRP recycling in the early endosome. *Embo j*. 2005;24(16):2851-2861.
16. Knauth P, Schluter T, Czubayko M, et al. Functions of sorting nexin 17 domains and recognition motif for P-selectin trafficking. *J Mol Biol*. 2005;347(4):813-825.
17. Adachi H, Tsujimoto M. Adaptor protein sorting nexin 17 interacts with the scavenger receptor FEEL-1/stabilin-1 and modulates its expression on the cell surface. *Biochim Biophys Acta*. 2010;1803(5):553-563.
18. Lee J, Retamal C, Cuitino L, et al. Adaptor protein sorting nexin 17 regulates amyloid precursor protein trafficking and processing in the early endosomes. *J Biol Chem*. 2008;283(17):11501-11508.
19. Steinberg F, Heesom KJ, Bass MD, Cullen PJ. SNX17 protects integrins from degradation by sorting between lysosomal and recycling pathways. *J Cell Biol*. 2012;197(2):219-230.
20. Bottcher RT, Stremmel C, Meves A, et al. Sorting nexin 17 prevents lysosomal degradation of beta1 integrins by binding to the beta1-integrin tail. *Nat Cell Biol*. 2012;14(6):584-592.
21. Chen KE, Healy MD, Collins BM. Towards a molecular understanding of endosomal trafficking by Retromer and Retriever. *Traffic*. 2019;20(7):465-478.

22. Tseng HY, Thorausch N, Ziegler T, Meves A, Fassler R, Bottcher RT. Sorting nexin 31 binds multiple beta integrin cytoplasmic domains and regulates beta1 integrin surface levels and stability. *J Mol Biol.* 2014;426(18):3180-3194.
23. Lauffer BE, Melero C, Temkin P, et al. SNX27 mediates PDZ-directed sorting from endosomes to the plasma membrane. *J Cell Biol.* 2010;190(4):565-574.
24. Loo LS, Tang N, Al-Haddawi M, Dawe GS, Hong W. A role for sorting nexin 27 in AMPA receptor trafficking. *Nat Commun.* 2014;5:3176.
25. Balana B, Maslennikov I, Kwiatkowski W, et al. Mechanism underlying selective regulation of G protein-gated inwardly rectifying potassium channels by the psychostimulant-sensitive sorting nexin 27. *Proc Natl Acad Sci U S A.* 2011;108(14):5831-5836.
26. Zimmerman SP, Hueschen CL, Malide D, Milgram SL, Playford MP. Sorting nexin 27 (SNX27) associates with zonula occludens-2 (ZO-2) and modulates the epithelial tight junction. *Biochem J.* 2013;455(1):95-106.
27. Soulet F, Yarar D, Leonard M, Schmid SL. SNX9 Regulates Dynamin Assembly and Is Required for Efficient Clathrin-mediated Endocytosis. *Mol Biol Cell.* 2005;16(4):2058-2067.
28. Yarar D, Waterman-Storer CM, Schmid SL. SNX9 couples actin assembly to phosphoinositide signals and is required for membrane remodeling during endocytosis. *Dev Cell.* 2007;13(1):43-56.
29. Burd C, Cullen PJ. Retromer: A Master Conductor of Endosome Sorting. In: *Cold Spring Harb Perspect Biol.* Vol 6.2014.
30. Seaman MN. Cargo-selective endosomal sorting for retrieval to the Golgi requires retromer. *J Cell Biol.* 2004;165(1):111-122.
31. Arighi CN, Hartnell LM, Aguilar RC, Haft CR, Bonifacino JS. Role of the mammalian retromer in sorting of the cation-independent mannose 6-phosphate receptor. *J Cell Biol.* 2004;165(1):123-133.

32. Temkin P, Lauffer B, Jager S, Cimermancic P, Krogan NJ, von Zastrow M. SNX27 mediates retromer tubule entry and endosome-to-plasma membrane trafficking of signalling receptors. *Nat Cell Biol.* 2011;13(6):715-721.
33. Vilarino-Guell C, Wider C, Ross OA, et al. VPS35 mutations in Parkinson disease. *Am J Hum Genet.* 2011;89(1):162-167.
34. Zimprich A, Benet-Pages A, Struhal W, et al. A mutation in VPS35, encoding a subunit of the retromer complex, causes late-onset Parkinson disease. *Am J Hum Genet.* 2011;89(1):168-175.
35. Small SA, Kent K, Pierce A, et al. Model-guided microarray implicates the retromer complex in Alzheimer's disease. *Ann Neurol.* 2005;58(6):909-919.
36. Norwood SJ, Shaw DJ, Cowieson NP, Owen DJ, Teasdale RD, Collins BM. Assembly and solution structure of the core retromer protein complex. *Traffic.* 2011;12(1):56-71.
37. Swarbrick JD, Shaw DJ, Chhabra S, et al. VPS29 is not an active metallo-phosphatase but is a rigid scaffold required for retromer interaction with accessory proteins. *PLoS One.* 2011;6(5):e20420.
38. Collins BM, Skinner CF, Watson PJ, Seaman MN, Owen DJ. Vps29 has a phosphoesterase fold that acts as a protein interaction scaffold for retromer assembly. *Nat Struct Mol Biol.* 2005;12(7):594-602.
39. Hierro A, Rojas AL, Rojas R, et al. Functional architecture of the retromer cargo-recognition complex. *Nature.* 2007;449(7165):1063-1067.
40. Priya A, Kalaidzidis IV, Kalaidzidis Y, Lambright D, Datta S. Molecular insights into Rab7-mediated endosomal recruitment of core retromer: deciphering the role of Vps26 and Vps35. *Traffic.* 2015;16(1):68-84.
41. Seaman MN, Harbour ME, Tattersall D, Read E, Bright N. Membrane recruitment of the cargo-selective retromer subcomplex is catalysed by the small GTPase Rab7 and inhibited by the Rab-GAP TBC1D5. *J Cell Sci.* 2009;122(Pt 14):2371-2382.

42. Haft CR, de la Luz Sierra M, Barr VA, Haft DH, Taylor SI. Identification of a family of sorting nexin molecules and characterization of their association with receptors. *Mol Cell Biol.* 1998;18(12):7278-7287.
43. Xu Y, Hortsman H, Seet L, Wong SH, Hong W. SNX3 regulates endosomal function through its PX-domain-mediated interaction with PtdIns(3)P. *Nat Cell Biol.* 2001;3(7):658-666.
44. Harrison MS, Hung CS, Liu TT, Christiano R, Walther TC, Burd CG. A mechanism for retromer endosomal coat complex assembly with cargo. *Proc Natl Acad Sci U S A.* 2014;111(1):267-272.
45. Harterink M, Port F, Lorenowicz MJ, et al. A SNX3-dependent retromer pathway mediates retrograde transport of the Wnt sorting receptor Wntless and is required for Wnt secretion. *Nat Cell Biol.* 2011;13(8):914-923.
46. Zhang P, Wu Y, Belenkaya TY, Lin X. SNX3 controls Wingless/Wnt secretion through regulating retromer-dependent recycling of Wntless. *Cell Res.* 2011;21(12):1677-1690.
47. MacDonald BT, Tamai K, He X. Wnt/beta-catenin signaling: components, mechanisms, and diseases. *Dev Cell.* 2009;17(1):9-26.
48. Das S, Yu S, Sakamori R, et al. Rab8a vesicles regulate Wnt ligand delivery and Paneth cell maturation at the intestinal stem cell niche. *Development.* 2015;142(12):2147-2162.
49. Cadigan KM, Waterman ML. TCF/LEFs and Wnt signaling in the nucleus. *Cold Spring Harb Perspect Biol.* 2012;4(11).
50. Clevers H. Wnt/beta-catenin signaling in development and disease. *Cell.* 2006;127(3):469-480.
51. Chen C, Garcia-Santos D, Ishikawa Y, et al. Snx3 regulates recycling of the transferrin receptor and iron assimilation. *Cell Metab.* 2013;17(3):343-352.
52. Lucas M, Gershlick DC, Vidaurrezaga A, Rojas AL, Bonifacino JS, Hierro A. Structural Mechanism for Cargo Recognition by the Retromer Complex. *Cell.* 2016;167(6):1623-1635.e1614.

53. Duan G, Walther D. The Roles of Post-translational Modifications in the Context of Protein Interaction Networks. *PLoS Comput Biol.* 2015;11(2).
54. Walsh CT, Garneau-Tsodikova S, Gatto GJ, Jr. Protein posttranslational modifications: the chemistry of proteome diversifications. *Angew Chem Int Ed Engl.* 2005;44(45):7342-7372.
55. Omenn GS, Lane L, Lundberg EK, Beavis RC, Overall CM, Deutsch EW. Metrics for the Human Proteome Project 2016: Progress on Identifying and Characterizing the Human Proteome, Including Post-Translational Modifications. *J Proteome Res.* 2016;15(11):3951-3960.
56. Cohen P. The origins of protein phosphorylation. *Nat Cell Biol.* 2002;4(5):E127-130.
57. Humphrey SJ, James DE, Mann M. Protein Phosphorylation: A Major Switch Mechanism for Metabolic Regulation. *Trends Endocrinol Metab.* 2015;26(12):676-687.
58. Hunter T. Protein kinases and phosphatases: the yin and yang of protein phosphorylation and signaling. *Cell.* 1995;80(2):225-236.
59. Lim YP. Mining the tumor phosphoproteome for cancer markers. *Clin Cancer Res.* 2005;11(9):3163-3169.
60. Singh V, Ram M, Kumar R, Prasad R, Roy BK, Singh KK. Phosphorylation: Implications in Cancer. *Protein J.* 2017;36(1):1-6.
61. Lenoir M, Ustunel C, Rajesh S, et al. Phosphorylation of conserved phosphoinositide binding pocket regulates sorting nexin membrane targeting. *Nat Commun.* 2018;9(1):993.
62. Hoffert JD, Pisitkun T, Wang G, Shen RF, Knepper MA. Quantitative phosphoproteomics of vasopressin-sensitive renal cells: regulation of aquaporin-2 phosphorylation at two sites. *Proc Natl Acad Sci U S A.* 2006;103(18):7159-7164.
63. Villén J, Beausoleil SA, Gerber SA, Gygi SP. Large-scale phosphorylation analysis of mouse liver. *Proc Natl Acad Sci U S A.* 2007;104(5):1488-1493.

64. Palacios-Moreno J, Foltz L, Guo A, et al. Neuroblastoma tyrosine kinase signaling networks involve FYN and LYN in endosomes and lipid rafts. *PLoS Comput Biol.* 2015;11(4):e1004130.
65. Mertins P, Mani DR, Ruggles KV, et al. Proteogenomics connects somatic mutations to signalling in breast cancer. *Nature.* 2016;534(7605):55-62.
66. Weber C, Schreiber TB, Daub H. Dual phosphoproteomics and chemical proteomics analysis of erlotinib and gefitinib interference in acute myeloid leukemia cells. *J Proteomics.* 2012;75(4):1343-1356.
67. Rolland D, Basrur V, Conlon K, et al. Global phosphoproteomic profiling reveals distinct signatures in B-cell non-Hodgkin lymphomas. *Am J Pathol.* 2014;184(5):1331-1342.
68. Stringer DK, Piper RC. Terminating protein ubiquitination: Hasta la vista, ubiquitin. *Cell Cycle.* 2011;10(18):3067-3071.
69. Technology CS. Ubiquitin / Proteasome. Published 2019. Accessed.
70. Schnell JD, Hicke L. Non-traditional functions of ubiquitin and ubiquitin-binding proteins. *J Biol Chem.* 2003;278(38):35857-35860.
71. Jin L, Williamson A, Banerjee S, Philipp I, Rape M. Mechanism of ubiquitin-chain formation by the human anaphase-promoting complex. *Cell.* 2008;133(4):653-665.
72. Pickart CM. Mechanisms underlying ubiquitination. *Annu Rev Biochem.* 2001;70:503-533.
73. Haglund K, Sigismund S, Polo S, Szymkiewicz I, Di Fiore PP, Dikic I. Multiple monoubiquitination of RTKs is sufficient for their endocytosis and degradation. *Nat Cell Biol.* 2003;5(5):461-466.
74. Hicke L. Protein regulation by monoubiquitin. *Nature Reviews Molecular Cell Biology.* 2019;2(3):195-201.
75. Boulkroun S, Ruffieux-Daidie D, Vitagliano JJ, et al. Vasopressin-inducible ubiquitin-specific protease 10 increases ENaC cell surface expression by deubiquitylating and stabilizing sorting nexin 3. *Am J Physiol Renal Physiol.* 2008;295(4):F889-900.

76. Lemmon MA, Schlessinger J, Ferguson KM. The EGFR family: not so prototypical receptor tyrosine kinases. *Cold Spring Harb Perspect Biol.* 2014;6(4):a020768.
77. Schlessinger J. Receptor tyrosine kinases: legacy of the first two decades. *Cold Spring Harb Perspect Biol.* 2014;6(3).
78. Yarden Y, Pines G. The ERBB network: at last, cancer therapy meets systems biology. *Nat Rev Cancer.* 2012;12(8):553-563.
79. Singh AB, Harris RC. Autocrine, paracrine and juxtacrine signaling by EGFR ligands. *Cell Signal.* 2005;17(10):1183-1193.
80. Macdonald-Obermann JL, Pike LJ. Different epidermal growth factor (EGF) receptor ligands show distinct kinetics and biased or partial agonism for homodimer and heterodimer formation. *J Biol Chem.* 2014;289(38):26178-26188.
81. Roepstorff K, Grandal MV, Henriksen L, et al. Differential Effects of EGFR Ligands on Endocytic Sorting of the Receptor. *Traffic.* 2009;10(8):1115-1127.
82. Lemmon MA, Schlessinger J. Cell signaling by receptor tyrosine kinases. *Cell.* 2010;141(7):1117-1134.
83. Huang F, Kirkpatrick D, Jiang X, Gygi S, Sorkin A. Differential regulation of EGF receptor internalization and degradation by multiubiquitination within the kinase domain. *Mol Cell.* 2006;21(6):737-748.
84. Kovacs E, Zorn JA, Huang Y, Barros T, Kuriyan J. A structural perspective on the regulation of the epidermal growth factor receptor. *Annu Rev Biochem.* 2015;84:739-764.
85. Chung I, Akita R, Vandlen R, Toomre D, Schlessinger J, Mellman I. Spatial control of EGF receptor activation by reversible dimerization on living cells. *Nature.* 2010;464(7289):783-787.
86. Caldieri G, Malabarba MG, Di Fiore PP, Sigismund S. EGFR Trafficking in Physiology and Cancer. *Prog Mol Subcell Biol.* 2018;57:235-272.

87. Levkowitz G, Klapper LN, Tzahar E, Freywald A, Sela M, Yarden Y. Coupling of the c-Cbl protooncogene product to ErbB-1/EGF-receptor but not to other ErbB proteins. *Oncogene*. 1996;12(5):1117-1125.
88. Lenferink AE, Pinkas-Kramarski R, van de Poll ML, et al. Differential endocytic routing of homo- and hetero-dimeric ErbB tyrosine kinases confers signaling superiority to receptor heterodimers. *Embo j*. 1998;17(12):3385-3397.
89. Sigismund S, Algisi V, Nappo G, et al. Threshold-controlled ubiquitination of the EGFR directs receptor fate. *Embo j*. 2013;32(15):2140-2157.
90. Vieira AV, Lamaze C, Schmid SL. Control of EGF receptor signaling by clathrin-mediated endocytosis. *Science*. 1996;274(5295):2086-2089.
91. Sigismund S, Woelk T, Puri C, et al. Clathrin-independent endocytosis of ubiquitinated cargos. *Proc Natl Acad Sci U S A*. 2005;102(8):2760-2765.
92. Kurten RC, Cadena DL, Gill GN. Enhanced degradation of EGF receptors by a sorting nexin, SNX1. *Science*. 1996;272(5264):1008-1010.
93. Gullapalli A, Garrett TA, Paing MM, Griffin CT, Yang Y, Trejo J. A Role for Sorting Nexin 2 in Epidermal Growth Factor Receptor Down-regulation: Evidence for Distinct Functions of Sorting Nexin 1 and 2 in Protein Trafficking. *Mol Biol Cell*. 2004;15(5):2143-2155.
94. Cavet ME, Pang J, Yin G, Berk BC. An epidermal growth factor (EGF) - dependent interaction between GIT1 and sorting nexin 6 promotes degradation of the EGF receptor. *Faseb j*. 2008;22(10):3607-3616.
95. Choi JH, Hong WP, Kim MJ, Kim JH, Ryu SH, Suh PG. Sorting nexin 16 regulates EGF receptor trafficking by phosphatidylinositol-3-phosphate interaction with the Phox domain. *J Cell Sci*. 2004;117(Pt 18):4209-4218.
96. Qin B, He M, Chen X, Pei D. Sorting nexin 10 induces giant vacuoles in mammalian cells. *J Biol Chem*. 2006;281(48):36891-36896.
97. Liu H, Liu ZQ, Chen CX, Magill S, Jiang Y, Liu YJ. Inhibitory regulation of EGF receptor degradation by sorting nexin 5. *Biochem Biophys Res Commun*. 2006;342(2):537-546.

98. Zhou Q, Huang T, Jiang Z, et al. Upregulation of SNX5 predicts poor prognosis and promotes hepatocellular carcinoma progression by modulating the EGFR-ERK1/2 signaling pathway. *Oncogene*. 2019.
99. Simonetti B, Paul B, Chaudhari K, et al. Molecular identification of a BAR domain-containing coat complex for endosomal recycling of transmembrane proteins. *Nat Cell Biol*. 2019;21(10):1219-1233.
100. Ghai R, Mobli M, Collins BM. Measuring interactions of FERM domain-containing sorting Nexin proteins with endosomal lipids and cargo molecules. *Methods Enzymol*. 2014;534:331-349.
101. Simonetti B, Danson CM, Heesom KJ, Cullen PJ. Sequence-dependent cargo recognition by SNX-BARs mediates retromer-independent transport of CI-MPR. *J Cell Biol*. 2017;216(11):3695-3712.
102. Cui Y, Carosi JM, Yang Z, et al. Retromer has a selective function in cargo sorting via endosome transport carriers. *J Cell Biol*. 2019;218(2):615-631.
103. Wendt MK, Williams WK, Pascuzzi PE, et al. The antitumorigenic function of EGFR in metastatic breast cancer is regulated by expression of Mig6. *Neoplasia*. 2015;17(1):124-133.
104. Lehmann BD, Pietenpol JA, Tan AR. Triple-negative breast cancer: molecular subtypes and new targets for therapy. *Am Soc Clin Oncol Educ Book*. 2015:e31-39.
105. Chiow KH, Tan Y, Chua RY, et al. SNX3-dependent regulation of epidermal growth factor receptor (EGFR) trafficking and degradation by aspirin in epidermoid carcinoma (A-431) cells. *Cell Mol Life Sci*. 2012;69(9):1505-1521.
106. Akman HB, Oyken M, Tuncer T, Can T, Erson-Bensan AE. 3'UTR shortening and EGF signaling: implications for breast cancer. *Hum Mol Genet*. 2015;24(24):6910-6920.
107. Maltseva DV, Khaustova NA, Fedotov NN, et al. High-throughput identification of reference genes for research and clinical RT-qPCR analysis of breast cancer samples. *J Clin Bioinforma*. 2013;3:13.

108. Fleige S, Walf V, Huch S, Prgomet C, Sehm J, Pfaffl MW. Comparison of relative mRNA quantification models and the impact of RNA integrity in quantitative real-time RT-PCR. *Biotechnol Lett.* 2006;28(19):1601-1613.
109. Rocha N, Kuijl C, van der Kant R, et al. Cholesterol sensor ORP1L contacts the ER protein VAP to control Rab7-RILP-p150 Glued and late endosome positioning. *J Cell Biol.* 2009;185(7):1209-1225.
110. Jongsma ML, Berlin I, Wijdeven RH, et al. An ER-Associated Pathway Defines Endosomal Architecture for Controlled Cargo Transport. *Cell.* 2016;166(1):152-166.
111. Pohl SG, Brook N, Agostino M, Arfuso F, Kumar AP, Dharmarajan A. Wnt signaling in triple-negative breast cancer. *Oncogenesis.* 2017;6(4):e310-.
112. Wee P, Wang Z. Epidermal Growth Factor Receptor Cell Proliferation Signaling Pathways. *Cancers (Basel).* 2017;9(5).
113. Doerr A. Proximity labeling with TurboID. *Nat Methods.* 2018;15(10):764.
114. Obenauer JC, Cantley LC, Yaffe MB. Scansite 2.0: Proteome-wide prediction of cell signaling interactions using short sequence motifs. *Nucleic Acids Res.* 2003;31(13):3635-3641.
115. Johannes L, Wunder C. The SNXy flavours of endosomal sorting. In: *Nat Cell Biol.* Vol 13. England 2011:884-886.
116. Howe LR, Brown AM. Wnt signaling and breast cancer. *Cancer Biol Ther.* 2004;3(1):36-41.
117. Masuda H, Zhang D, Bartholomeusz C, Doihara H, Hortobagyi GN, Ueno NT. Role of Epidermal Growth Factor Receptor in Breast Cancer. *Breast Cancer Res Treat.* 2012;136(2).

APPENDICES

A. Buffers and Solutions

10% Separating Gel Mix:

3.33 ml Acrylamide – Bisacrylamide (30%)

2.5 ml 1.5M Tris-HCl pH: 8.8

100 µl SDS (10%)

100 µl APS (10%)

4µl TEMED

3.96 ml dH₂O

5% Stacking Gel Mix:

1.36 ml Acrylamide – Bisacrylamide (30%)

1 ml 1M Tris-HCl pH: 6.8

80 µl SDS (10%)

80 µl APS (10%)

8 µl TEMED

5.44 ml dH₂O

TBS-T:

20 mM Tris

137 mM NaCl

0.1% Tween 20

pH: 7.6

6X Laemmli Buffer:

12% SDS

30% 2-mercaptoethanol

60% Glycerol

0.012% bromophenol blue

0.375 M Tris

Mild Stripping Buffer:

15g Glycine

1 g SDS

10 ml Tween 20

Adjust the pH to 2.2

Complete to 1 L with dH₂O

10X Running Buffer:

25 mM Tris base

190 mM Glycine

0.1% SDS

Dilute 1X with dH₂O prior to use.

Transfer Buffer:

200 ml Methanol

100 ml 10X Blotting Buffer

700 ml dH₂O

10 X Blotting Buffer:

30.3 g Trizma Base (0.25M)

144 g Glycine (1.92M)

pH: 8.3

10X PBS:

1.37 M NaCl

27 mM KCl

100 mM Na₂HPO₄

pH 7.4

Lysis buffer for proximity-based labelling assay:

0.8% NP-40

50 mM NaCl

50 mM Tris-HCl (pH 8.0)

5 mM MgCl₂

Wash buffer for proximity-based labelling assay:

0.8% NP-40

150 mM NaCl

50 mM Tris-HCl (pH 8.0)

0.5% SDS

5 mM MgCl₂

10X citrate saline buffer:

1.35 M KCl

0.15 M sodium citrate

Autoclaved

Diluted to 1X with Molecular Grade water

Cell staining buffer:

5 g BSA

250 mg sodium azide

500 ml 1X PBS

Lysis buffer 1 (for ubiquitination assay):

50mM Tris-HCl pH 7.5

150mM NaCl

5 mM ethylenediaminetetraacetic acid (EDTA)

0.5% Triton X-100

10mM N-methyl maleimide (general DUB inhibitor diluted in DMSO, freshly added)

Lysis buffer 2 (for ubiquitination assay):

100mM Tris-HCl, pH 8.0

1 mM EDTA

2% SDS

3X SDS sample loading buffer:

188 mM Tris-Cl (pH 6.8)

3% SDS

30% glycerol

0.01% bromophenol blue

20 mM DTT (freshly added)

2X SDS sample loading buffer:

Tris-Cl (100 mM, pH 6.8)

SDS (electrophoresis grade) (4%)

Bromophenol blue (0.2%)

Glycerol (20%)

10 mM DTT (freshly added)

B. Vector Maps

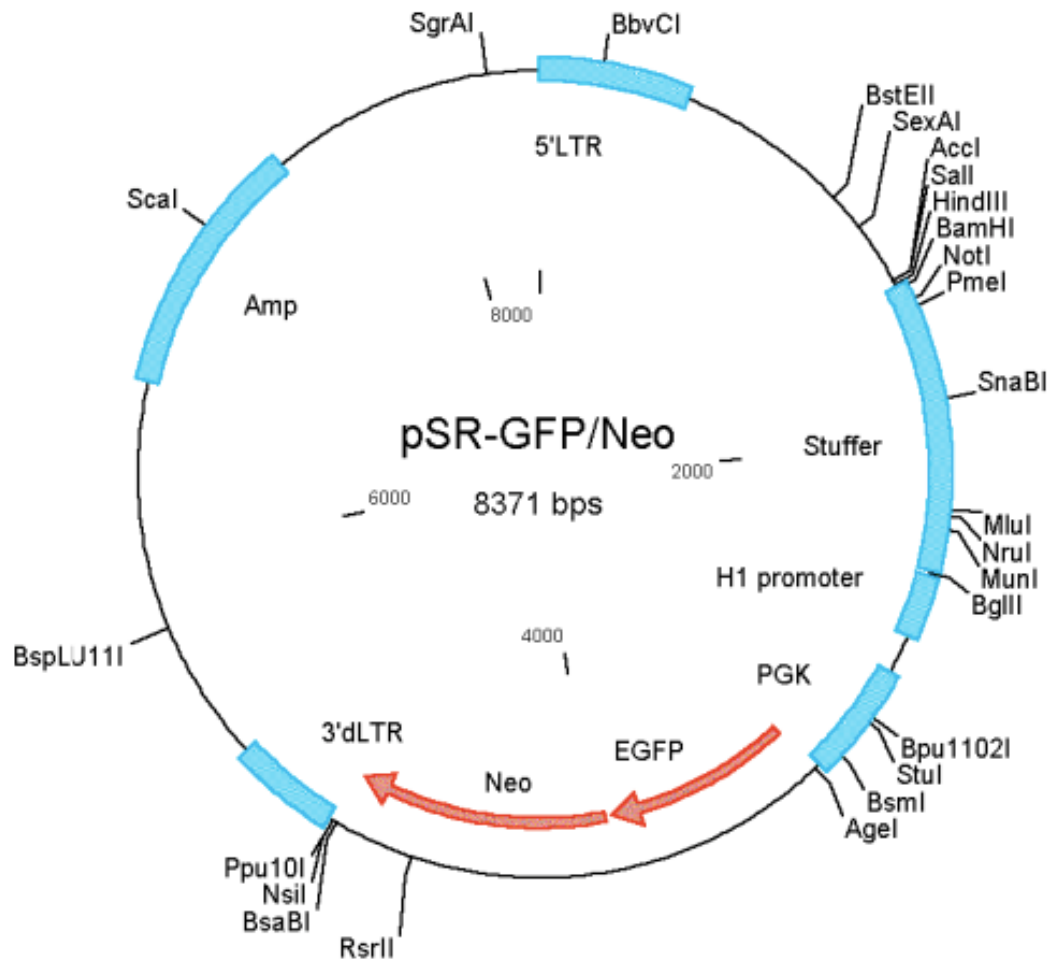


Figure B. 1 Vector map of pSUPER.retro.neo+GFP.

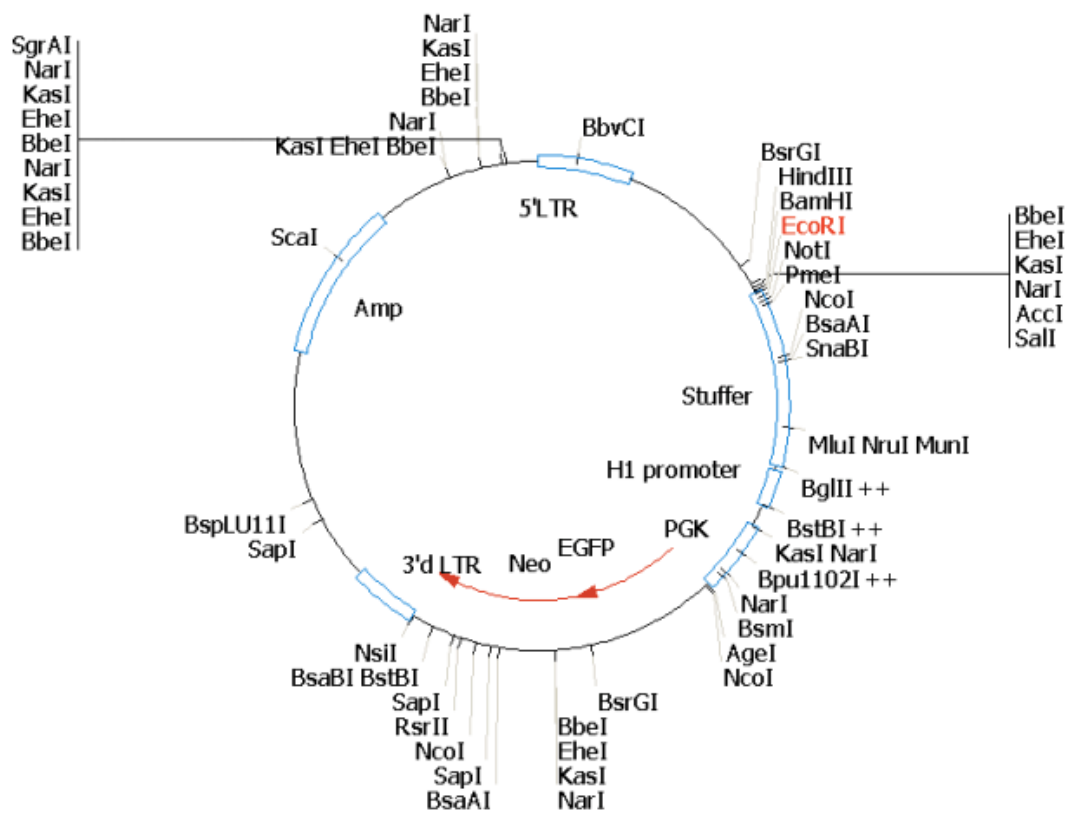


Figure B. 2 Vector map of pSUPERIOR.retro.neo+GFP

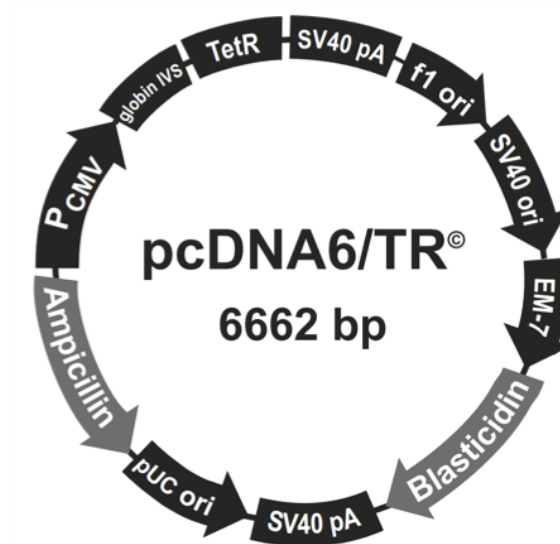


Figure B. 3 Vector map of pcDNA6/TR.

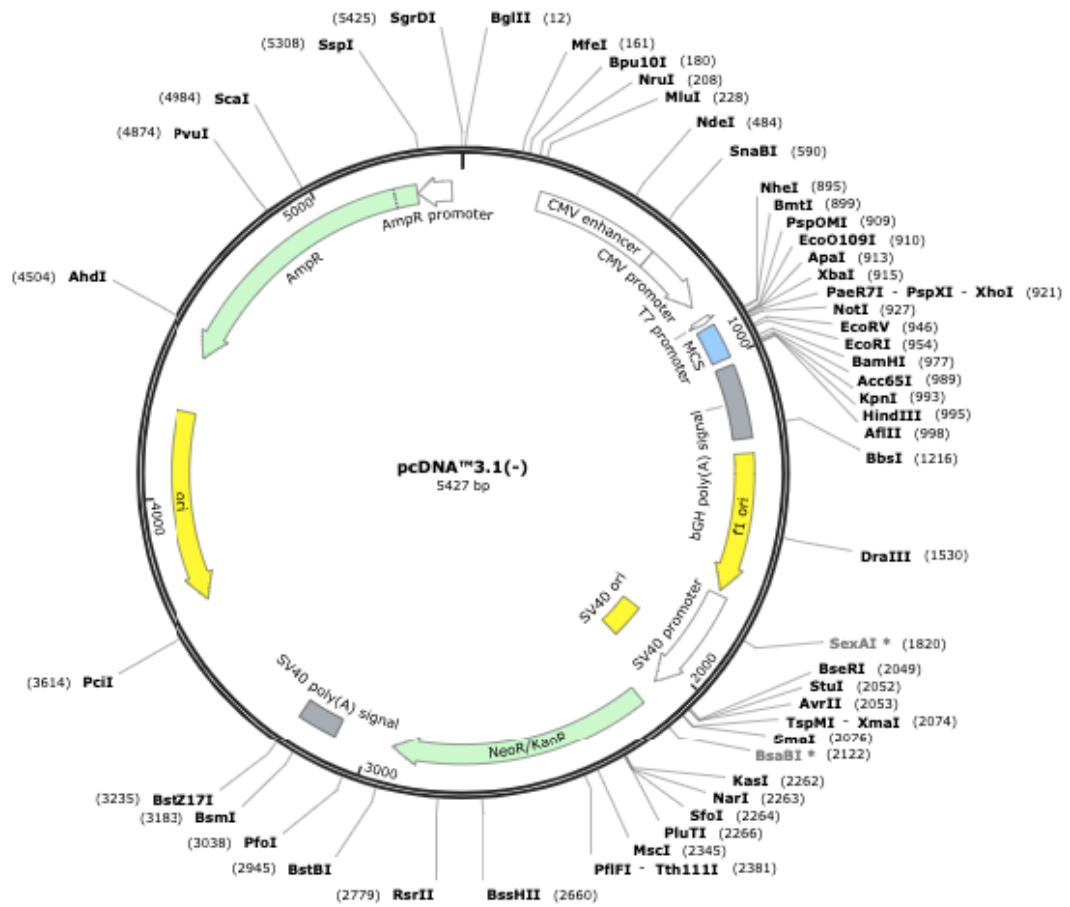


Figure B. 4 Vector map of pcDNA 3.1 (-).

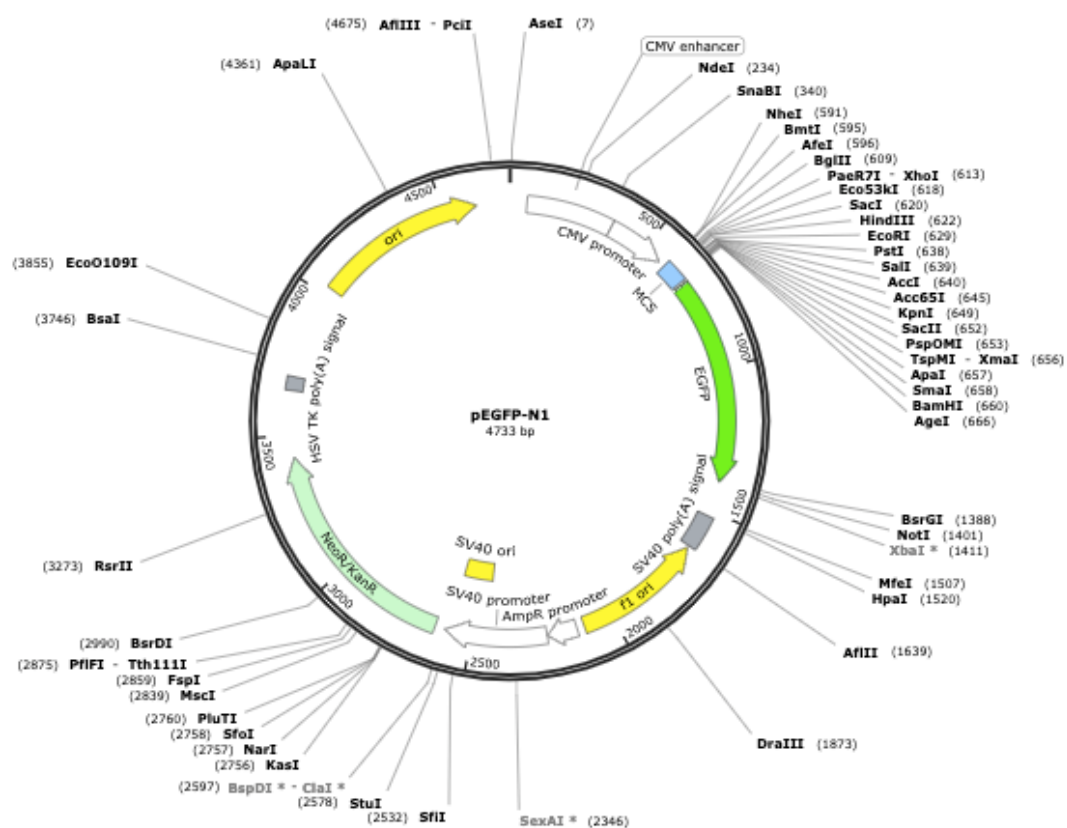


Figure B. 5 Vector map of pEGFP-N1.

C. Markers

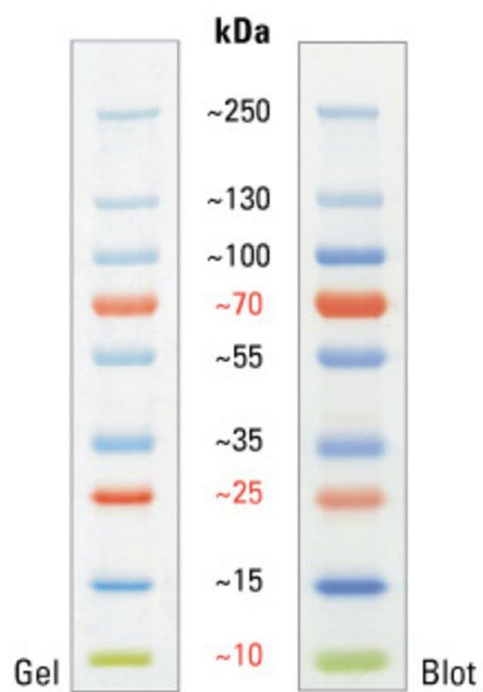


Figure C. 1 Protein ladder (Thermo PageRuler Plus Prestained, Cat #: 26619).

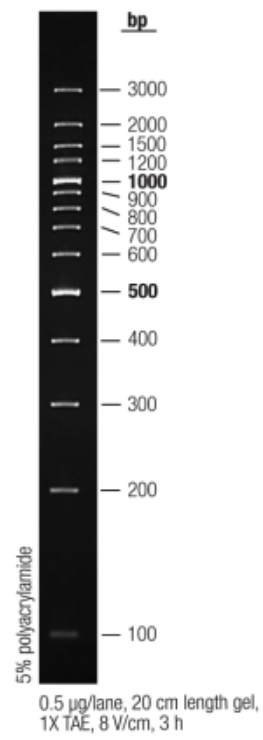


Figure C. 2 DNA Ladder (Thermo GeneRuler 100 bp Plus, Cat #: SM0321).

D. Sequence results of SNX3 mutants

Score	Expect	Identities	Gaps	Strand
868 bits(962)	0.0	484/486(99%)	0/486(0%)	Plus/Plus
Query 78	ATGGCGGAGACCGTGGCTGACACCCGGCGGCTGATCACCAAGCCGCAGAACCTGAATGAC	137		
Sbjct 120	ATGGCGGAGACCGTGGCTGACACCCGGCGGCTGATCACCAAGCCGCAGAACCTGAATGAC	179		
Query 138	GCCTACGGACCCCCCAGCAACTTCCTCGAGATCGATGTGAGCAACCCGCAAACGGTG	197		
Sbjct 180	GCCTACGGACCCCCCAGCAACTTCCTCGAGATCGATGTGAGCAACCCGCAAACGGTG	239		
Query 198	GTCGGCCGGGGCCGCTTACCACCTTACGAAATCAGGGTCAAGACAAATCTTCTATTTTC	257		
Sbjct 240	GTCGGCCGGGGCCGCTTACCACCTTACGAAATCAGGGTCAAGACAAATCTTCTATTTTC	299		
Query 258	AGGCTGAGAGAATCTACTGTTAGAAGAAGATACAGTGACTTTGAATGGCTGCGAAGTGAA	317		
Sbjct 300	AAGCTGAAAGAATCTACTGTTAGAAGAAGATACAGTGACTTTGAATGGCTGCGAAGTGAA	359		
Query 318	TTAGAAAGAGAGAGCAAGGTCGTAGTTCCCCCGCTCCCTGGGAAAGCGTTTTTGCCTCAG	377		
Sbjct 360	TTAGAAAGAGAGAGCAAGGTCGTAGTTCCCCCGCTCCCTGGGAAAGCGTTTTTGCCTCAG	419		
Query 378	CTTCCTTTTAGAGGAGATGATGGAATATTTGATGACAATTTTATTGAGGAAAGAAAACAA	437		
Sbjct 420	CTTCCTTTTAGAGGAGATGATGGAATATTTGATGACAATTTTATTGAGGAAAGAAAACAA	479		
Query 438	GGGCTGGAGCAGTTTATAAACAAGGTCGCTGGTCATCCTCTGGCACAGAACGAACGTTGT	497		
Sbjct 480	GGGCTGGAGCAGTTTATAAACAAGGTCGCTGGTCATCCTCTGGCACAGAACGAACGTTGT	539		
Query 498	CTTCACATGTTTTTACAAGATGAAATAATAGATAAAAGCTATACTCCATCTAAAATAAGA	557		
Sbjct 540	CTTCACATGTTTTTACAAGATGAAATAATAGATAAAAGCTATACTCCATCTAAAATAAGA	599		
Query 558	CATGCC 563			
Sbjct 600	CATGCC 605			

Figure D. 1 Sequence result of SNX3-GFP K61-63R mutant.

Score	Expect	Identities	Gaps	Strand	
873 bits(967)	0.0	485/486(99%)	0/486(0%)	Plus/Plus	
Query	77	ATGGCGGAGACCGTGGCTGACACCCGGCGGCTGATCACCAAGCCGCAGAACCTGAATGAC			136
Sbjct	120	ATGGCGGAGACCGTGGCTGACACCCGGCGGCTGATCACCAAGCCGCAGAACCTGAATGAC			179
Query	137	GCCTACGGACCCCCCAGCAACTTCCTCGAGATCGATGTGAGCAACCCGCAAACGGTGGGG			196
Sbjct	180	GCCTACGGACCCCCCAGCAACTTCCTCGAGATCGATGTGAGCAACCCGCAAACGGTGGGG			239
Query	197	GTCGGCCGGGGCCGCTTACCACCTTACGAAATCAGGGTCAAGACAAATCTTCCTATTTTC			256
Sbjct	240	GTCGGCCGGGGCCGCTTACCACCTTACGAAATCAGGGTCAAGACAAATCTTCCTATTTTC			299
Query	257	AAGCTGAAAGAATCTACTGTTAGAAGAAGATACAGTGACTTTGAATGGCTGCGAAGTGAA			316
Sbjct	300	AAGCTGAAAGAATCTACTGTTAGAAGAAGATACAGTGACTTTGAATGGCTGCGAAGTGAA			359
Query	317	TTAGAAAGAGAGAGCAAGGTCGTAGTTCCTCCGCTCCCTGGGAGAGCGTTTTTGCCTCAG			376
Sbjct	360	TTAGAAAGAGAGAGCAAGGTCGTAGTTCCTCCGCTCCCTGGGAAAGCGTTTTTGCCTCAG			419
Query	377	CTTCCTTTTAGAGGAGATGATGGAATATTTGATGACAATTTTATTGAGGAAAGAAAACAA			436
Sbjct	420	CTTCCTTTTAGAGGAGATGATGGAATATTTGATGACAATTTTATTGAGGAAAGAAAACAA			479
Query	437	GGGCTGGAGCAGTTTATAACAAGGTCGCTGGTCATCCTCTGGCACAGAACGAACGTTGT			496
Sbjct	480	GGGCTGGAGCAGTTTATAACAAGGTCGCTGGTCATCCTCTGGCACAGAACGAACGTTGT			539
Query	497	CTTCACATGTTTTTACAAGATGAAATAATAGATAAAAAGCTATACTCCATCTAAAATAAGA			556
Sbjct	540	CTTCACATGTTTTTACAAGATGAAATAATAGATAAAAAGCTATACTCCATCTAAAATAAGA			599
Query	557	CATGCC			562
Sbjct	600	CATGCC			605

Figure D. 2 Sequence result of SNX3-GFP K95R mutant.

Score		Expect	Identities	Gaps	Strand
873 bits(967)		0.0	485/486(99%)	0/486(0%)	Plus/Plus
Query	76	ATGGCGGAGACCGTGGCTGACACCCGGCGGCTGATCACCAAGCCGCAGAACCTGAATGAC			135
Sbjct	120	ATGGCGGAGACCGTGGCTGACACCCGGCGGCTGATCACCAAGCCGCAGAACCTGAATGAC			179
Query	136	GCCTACGGACCCCCAGCAACTTCCTCGAGATCGATGTGAGCAACCCGCAAACGGTGGGG			195
Sbjct	180	GCCTACGGACCCCCAGCAACTTCCTCGAGATCGATGTGAGCAACCCGCAAACGGTGGGG			239
Query	196	GTCGGCCGGGGCCGCTTCACCACTTACGAAATCAGGGTCAAGACAAATCTTCCTATTTTC			255
Sbjct	240	GTCGGCCGGGGCCGCTTCACCACTTACGAAATCAGGGTCAAGACAAATCTTCCTATTTTC			299
Query	256	AAGCTGAAAGAATCTACTGTTAGAAGAAGATACAGTGACTTTGAATGGCTGCGAAGTGAA			315
Sbjct	300	AAGCTGAAAGAATCTACTGTTAGAAGAAGATACAGTGACTTTGAATGGCTGCGAAGTGAA			359
Query	316	TTAGAAAGAGAGAGCAAGGTCGTAGTTCCCCGCTCCCTGGGAAAGCGTTTTTGCCTCAG			375
Sbjct	360	TTAGAAAGAGAGAGCAAGGTCGTAGTTCCCCGCTCCCTGGGAAAGCGTTTTTGCCTCAG			419
Query	376	CTTCCTTTTAGAGGAGATGATGGAATATTTGATGACAATTTTATTGAGGAAAGAAGACAA			435
Sbjct	420	CTTCCTTTTAGAGGAGATGATGGAATATTTGATGACAATTTTATTGAGGAAAGAAAACAA			479
Query	436	GGGCTGGAGCAGTTTATAAACAAGGTCGCTGGTCATCCTCTGGCACAGAACGAACGTTGT			495
Sbjct	480	GGGCTGGAGCAGTTTATAAACAAGGTCGCTGGTCATCCTCTGGCACAGAACGAACGTTGT			539
Query	496	CTTCACATGTTTTTACAAGATGAAATAATAGATAAAAGCTATACTCCATCTAAAATAAGA			555
Sbjct	540	CTTCACATGTTTTTACAAGATGAAATAATAGATAAAAGCTATACTCCATCTAAAATAAGA			599
Query	556	CATGCC	561		
Sbjct	600	CATGCC	605		

Figure D. 3 Sequence result of SNX3-GFP K119R mutant.

Score	Expect	Identities	Gaps	Strand	
873 bits(967)	0.0	485/486(99%)	0/486(0%)	Plus/Plus	
Query 77	ATGGCGGAGACCGTGGCTGACACCCGGCGGCTGATCACCAAGCCGCAGAACCTGAATGAC	136			
Sbjct 120	ATGGCGGAGACCGTGGCTGACACCCGGCGGCTGATCACCAAGCCGCAGAACCTGAATGAC	179			
Query 137	GCCTACGGACCCCCCAGCAACTTCCTCGAGATCGATGTGAGCAACCCGCAAACGGTGGGG	196			
Sbjct 180	GCCTACGGACCCCCCAGCAACTTCCTCGAGATCGATGTGAGCAACCCGCAAACGGTGGGG	239			
Query 197	GTCGGCCGGGGCCGCTTCACCACTTACGAAATCAGGGTCAAGACAAATCTTCCTATTTTC	256			
Sbjct 240	GTCGGCCGGGGCCGCTTCACCACTTACGAAATCAGGGTCAAGACAAATCTTCCTATTTTC	299			
Query 257	AAGCTGAAAGAATCTACTGTTAGAAGAAGATACAGTGACTTTGAATGGCTGCGAAGTGAA	316			
Sbjct 300	AAGCTGAAAGAATCTACTGTTAGAAGAAGATACAGTGACTTTGAATGGCTGCGAAGTGAA	359			
Query 317	TTAGAAAGAGAGAGCAAGGTCGTAGTTCCCCCGCTCCCTGGGAAAGCGTTTTTTCGCTCAG	376			
Sbjct 360	TTAGAAAGAGAGAGCAAGGTCGTAGTTCCCCCGCTCCCTGGGAAAGCGTTTTTTCGCTCAG	419			
Query 377	CTTCCTTTTAGAGGAGATGATGGAATATTTGATGACAATTTTATTGAGGAAAGAAAACAA	436			
Sbjct 420	CTTCCTTTTAGAGGAGATGATGGAATATTTGATGACAATTTTATTGAGGAAAGAAAACAA	479			
Query 437	GGGCTGGAGCAGTTTATAAACAGGGTCGCTGGTCATCCTCTGGCACAGAACGAACGTTGT	496			
Sbjct 480	GGGCTGGAGCAGTTTATAAACAGGGTCGCTGGTCATCCTCTGGCACAGAACGAACGTTGT	539			
Query 497	CTTCACATGTTTTTACAAGATGAAATAATAGATAAAAGCTATACTCCATCTAAAATAAGA	556			
Sbjct 540	CTTCACATGTTTTTACAAGATGAAATAATAGATAAAAGCTATACTCCATCTAAAATAAGA	599			
Query 557	CATGCC 562				
Sbjct 600	CATGCC 605				

Figure D. 4 Sequence result of SNX3-GFP K128R mutant.

E. Flow cytometry

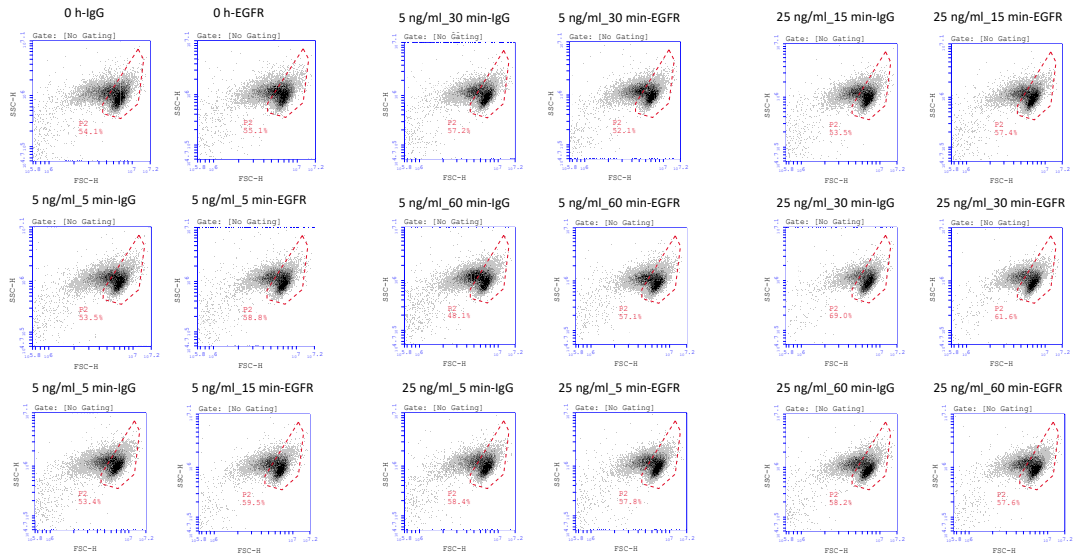


Figure E. 1 Gating strategy of the flow cytometry analysis.

CURRICULUM VITAE

PERSONAL INFORMATION

Surname, Name: Öyken, Merve
Nationality: Turkish (TC)
Date and Place of Birth: 27 October 1988, Selçuklu
Marital Status: Single
Phone: +90 312 210 50 44
email: moyken@metu.edu.tr

EDUCATION

Degree	Institution	Year of Graduation
MS	METU Biology	2014
BS	METU Biology	2011
High School	Meram Anatolian High School, Konya	2006

WORK EXPERIENCE

Year	Place	Enrollment
2014-2020	METU, Department of Biological Sciences	Research Assistant

FOREIGN LANGUAGES

Advanced English

PUBLICATIONS

1. Oguz Erdogan AS, Ozdemirler N, Oyken M, Alper M, Erson-Bensan AE, ARID3B expression in primary breast cancers and breast cancer-derived cell lines. "Cellular Oncology", 37, (2014), p.289-296.
2. Akman HB, Oyken M, Tuncer T, Can T, Erson-Bensan AE, 3'UTR shortening and EGF signaling: implications for breast cancer. "Human Molecular Genetics", 24, (2015), p.6910-6920.

3. Begik O, Oyken M, Cinkilli Alican T, Can T, Erson-Bensan AE, Alternative Polyadenylation Patterns for Novel Gene Discovery and Classification in Cancer. "Neoplasia", 19, (2017), p.574.
4. Yavuz E, Oyken M, Erson Bensan AE. ALCAM (Activated Leukocyte Cell Adhesion Molecule); "Atlas Genet Cytogenet Oncol Haematol.", (2017).
5. Oyken M, Erson-Bensan AE, mikroRNA'lar ve Kanser, In: Kanser Moleküler Biyolojisi, Edited by: Yusuf Baran. April 2018, Kısayol Yayıncılık, p197-208.